The American Journal of Human Genetics, Volume *106*

Supplemental Data

Allelic Heterogeneity at the *CRP* Locus Identified by Whole-Genome Sequencing in Multi-ancestry Cohorts

Laura M. Raffield, Apoorva K. Iyengar, Biqi Wang, Sheila M. Gaynor, Cassandra N. Spracklen, Xue Zhong, Madeline H. Kowalski, Shabnam Salimi, Linda M. Polfus, Emelia J. Benjamin, Joshua C. Bis, Russell Bowler, Brian E. Cade, Won Jung Choi, Alejandro P. Comellas, Adolfo Correa, Pedro Cruz, Harsha Doddapaneni, Peter Durda, Stephanie M. Gogarten, Deepti Jain, Ryan W. Kim, Brian G. Kral, Leslie A. Lange, Martin G. Larson, Cecelia Laurie, Jiwon Lee, Seonwook Lee, Joshua P. Lewis, Ginger A. Metcalf, Braxton D. Mitchell, Zeineen Momin, Donna M. Muzny, Nathan Pankratz, Cheol Joo Park, Stephen S. Rich, Jerome I. Rotter, Kathleen Ryan, Daekwan Seo, Russell P. Tracy, Karine A. Viaud-Martinez, Lisa R. Yanek, Lue Ping Zhao, Xihong Lin, Bingshan Li, Yun Li, Josée Dupuis, Alexander P. Reiner, Karen L. Mohlke, Paul L. Auer, TOPMed Inflammation Working Group, and NHLBI Trans-Omics for Precision Medicine (TOPMed) Consortium

Figure S1a: QQ-plot of association analysis for C-reactive protein in TOPMed.

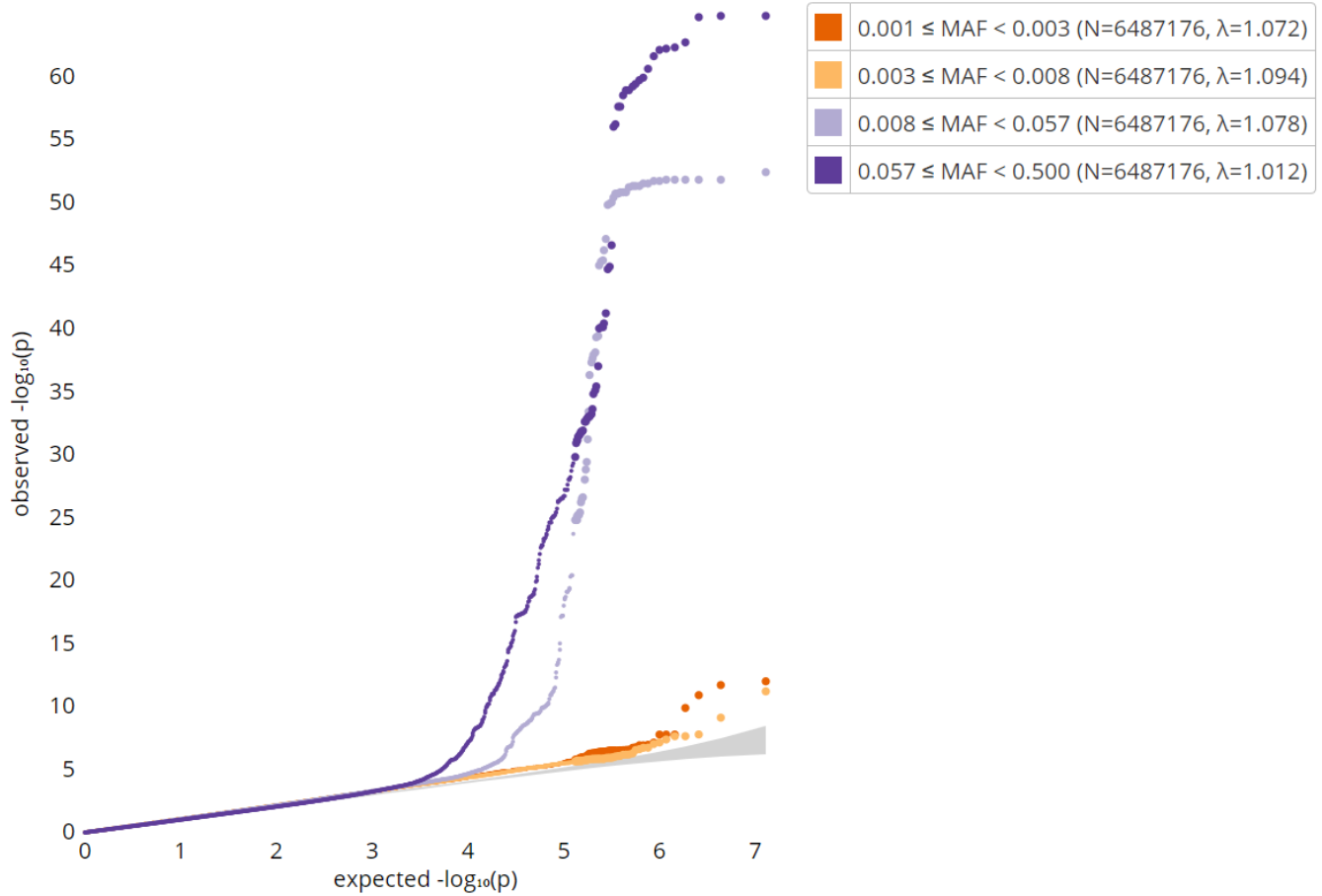

Observed versus expected $-\log_{10}$ p-values for all variants included in the pooled ancestry C-reactive protein analysis on ENCORE, stratified by minor allele frequency (MAF) bin, with genomic inflation λ for each bin.

Figure S1b: Manhattan plot of CRP association signals in TOPMed.

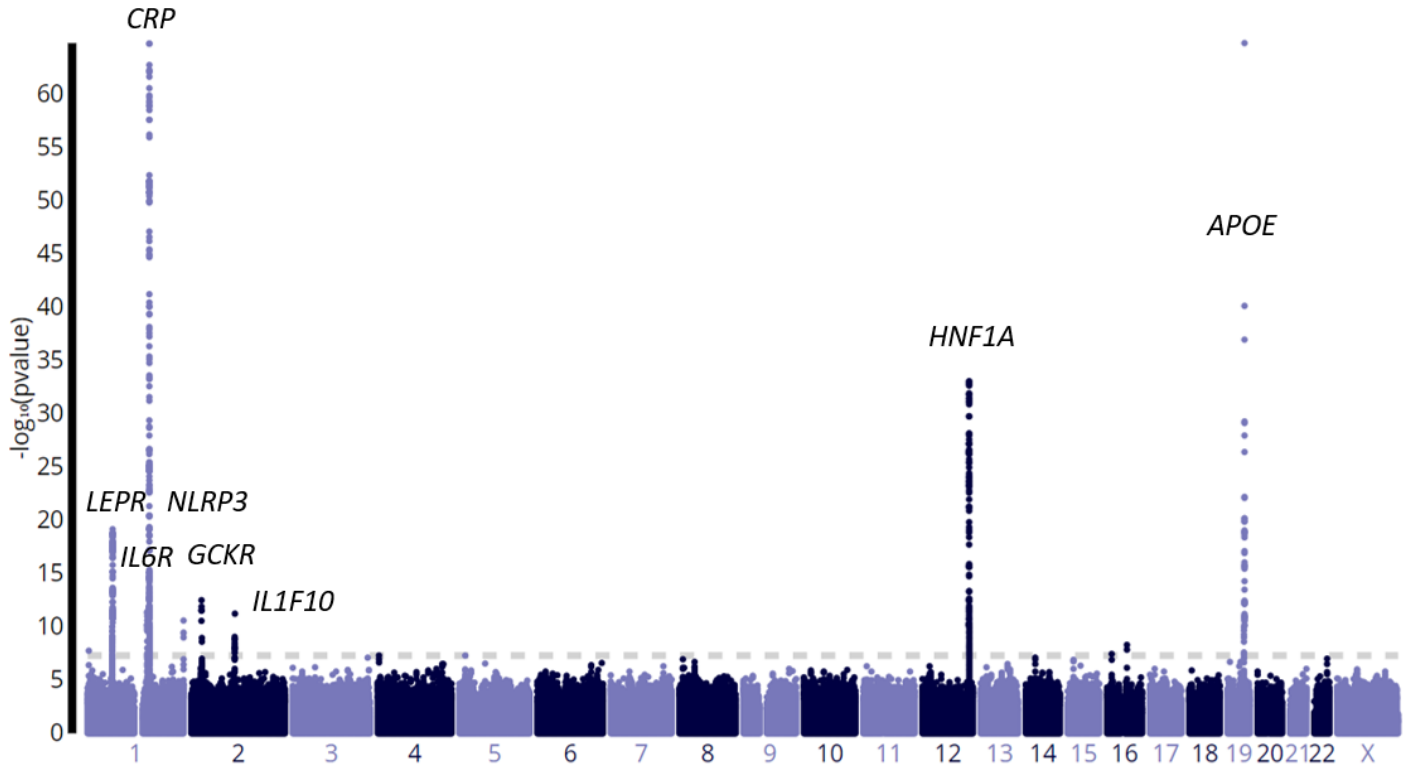

Y axis displays -$\log_{10}$ p-values for all variants included in the pooled ancestry C-reactive protein analysis on ENCORE, with the *x* axis displaying chromosomal position.

Figure S2: LocusZoom plots for sequential conditional analysis results at *CRP* locus, as well as plot of *CRP* locus adjusting for all previously identified *CRP* locus variants. For each plot, linkage disequilibrium is calculated using the same TOPMed samples included in our ancestry pooled C-reactive protein analyses.

a. In ancestry pooled analysis, LocusZoom plot of association results conditioned on rs7551731 (lead variant rs73024795). Letters in this and subsequent figures correspond to the list of conditionally distinct signals in Table 2. All plots display -log10(p-value) versus genomic location for all distinct signals subsequent to ones conditioned on, using order from Table. The lead variant for each conditionally distinct signal is indicated with a diamond, with other variants in linkage disequilibrium r^2>0.2 indicated in the colors used for each letter label and displayed on the legend at right, each with a different shape (for example, variants in close linkage disequilibrium with signal B (rs73024795) are displayed as pink triangles).

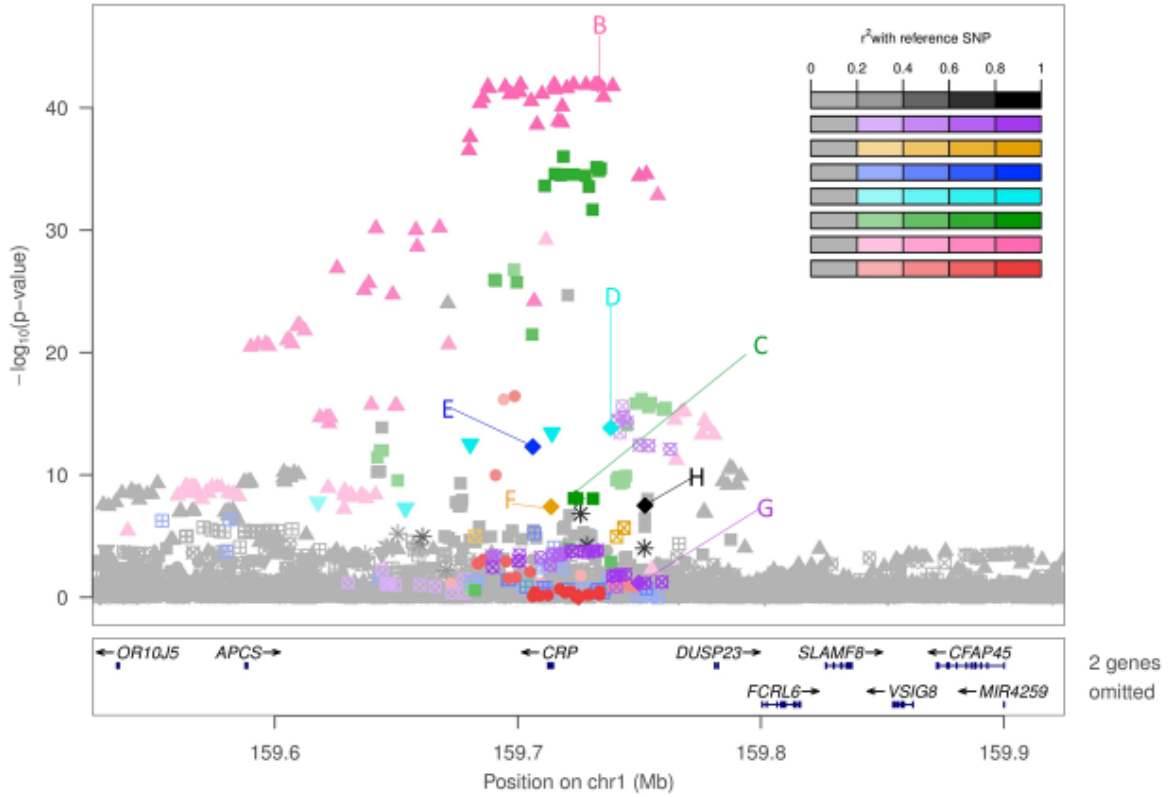

b. In ancestry pooled analysis, LocusZoom plot of association results conditioned on rs7551731 and rs73024795 (lead variant rs2211321).

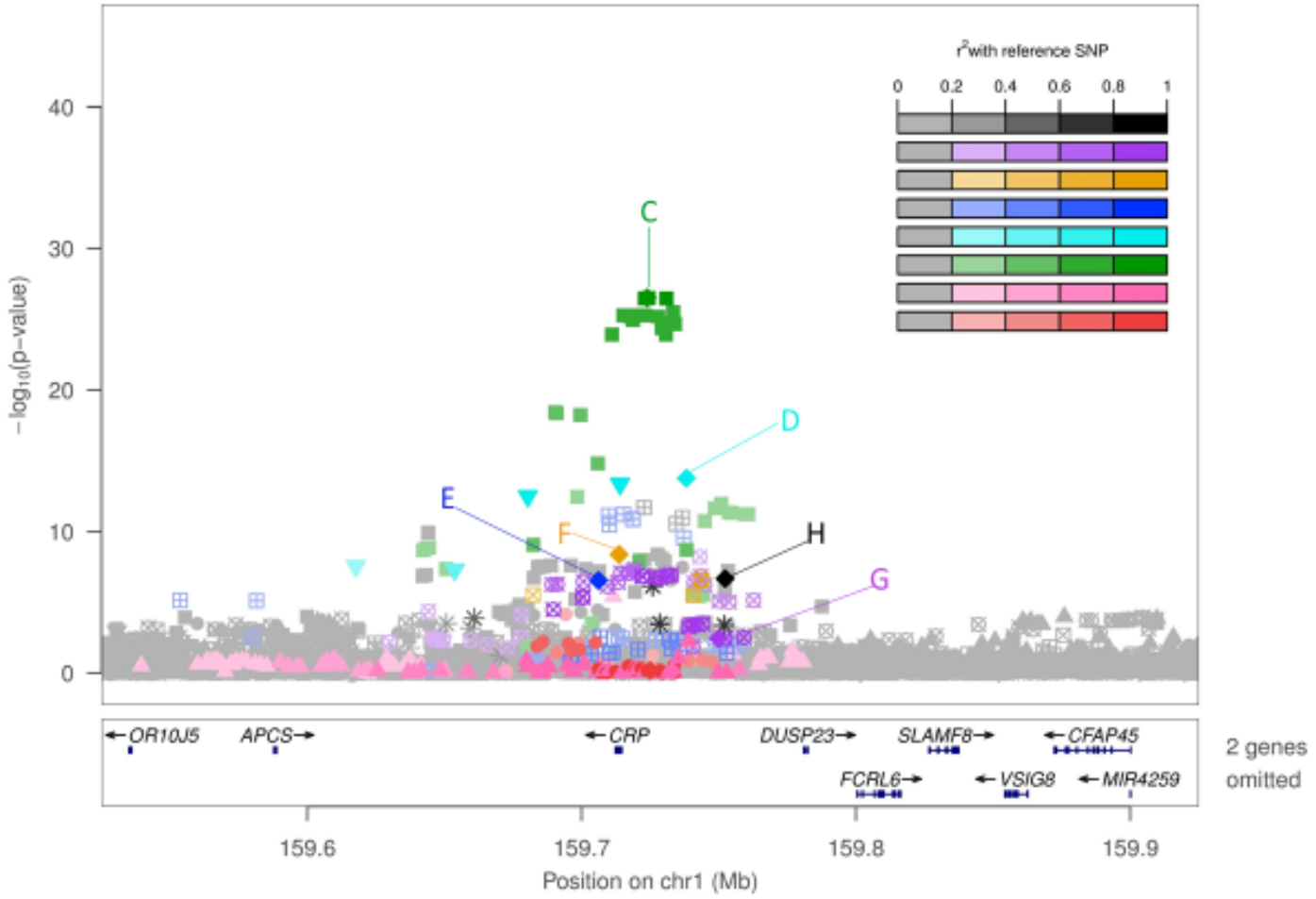

c. In ancestry pooled analysis, LocusZoom plot of association results conditioned on rs7551731, rs73024795, and rs2211321 (lead variant rs553202904).

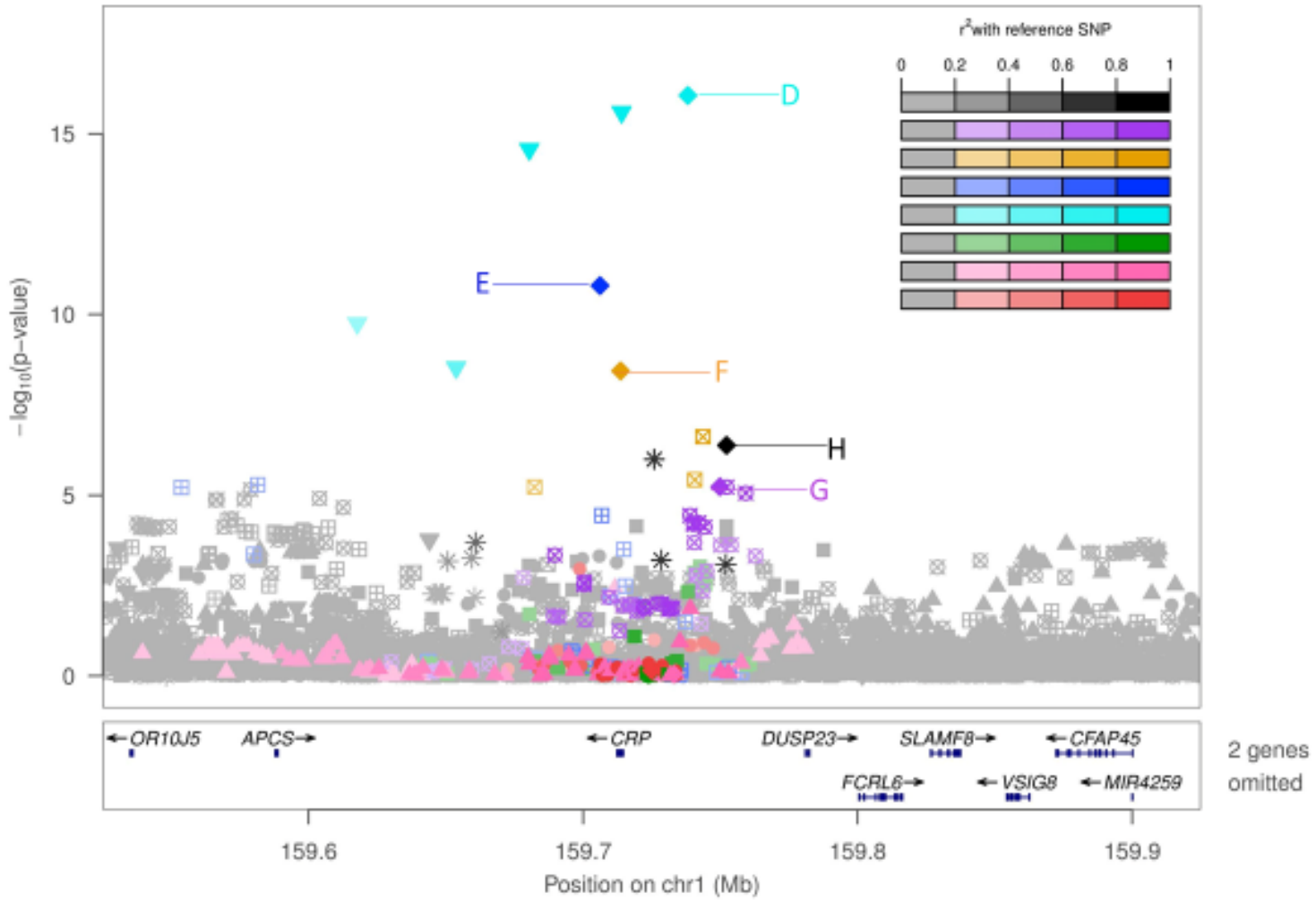

d. In ancestry pooled analysis, LocusZoom plot of association results conditioned on rs7551731, rs73024795, rs2211321, and rs553202904 (lead variant rs11265259).

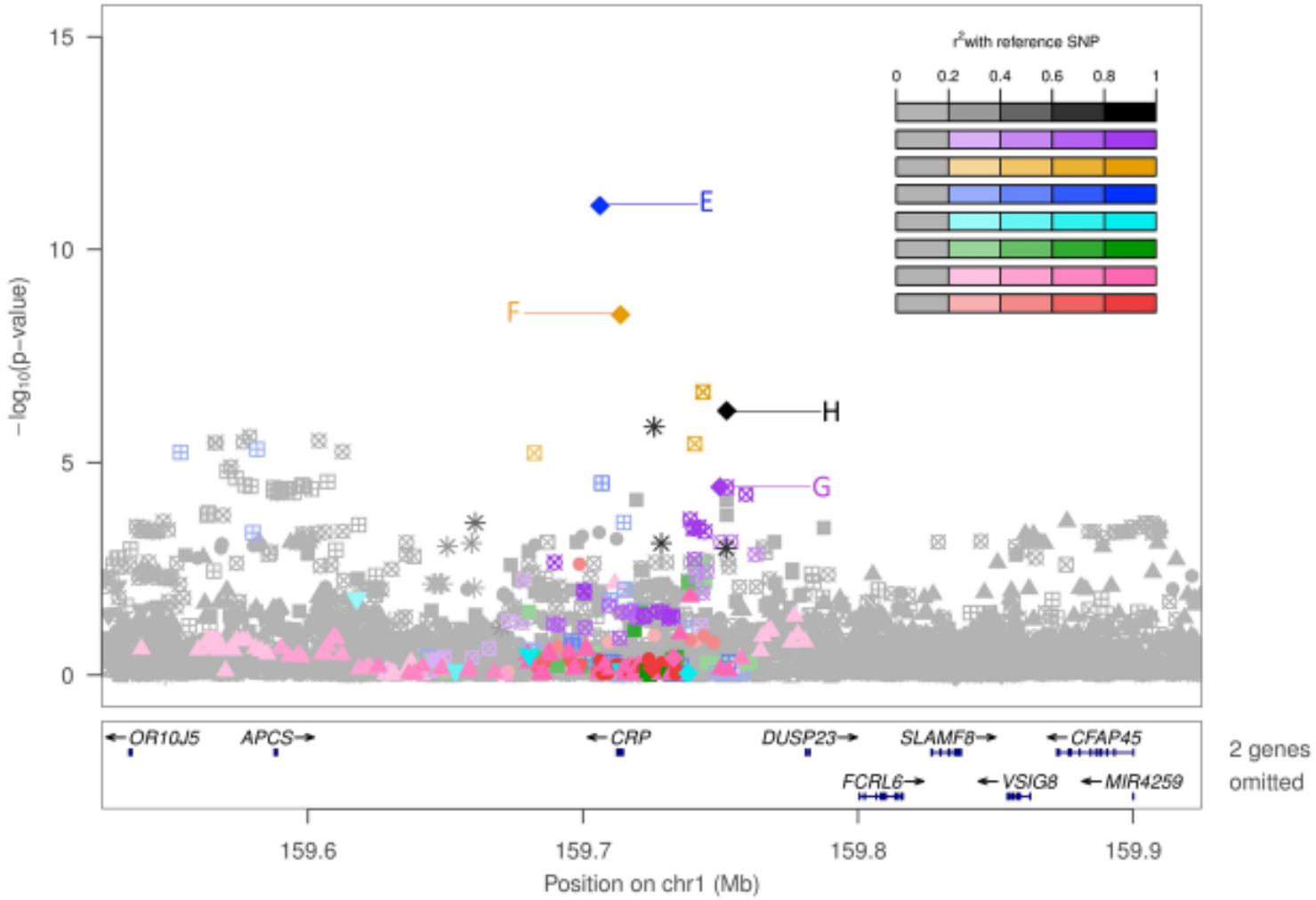

e. In ancestry pooled analysis, LocusZoom plot of association results conditioned on rs7551731, rs73024795, rs2211321, rs553202904, and rs11265259 (lead variant rs1800947).

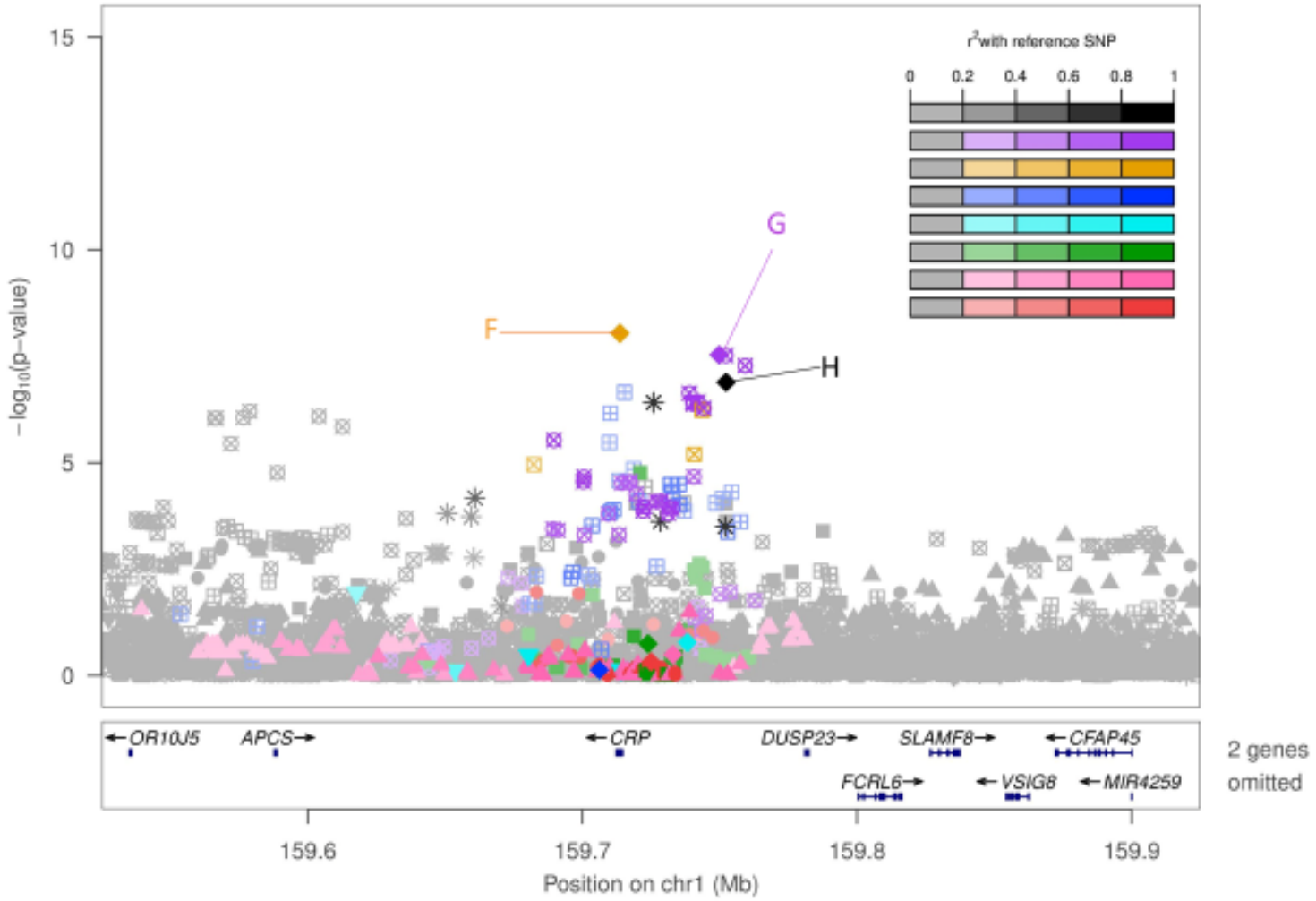

f. In ancestry pooled analysis, LocusZoom plot of association results conditioned on rs7551731, rs73024795, rs2211321, rs553202904, rs11265259, and rs1800947 (lead variant rs12734907).

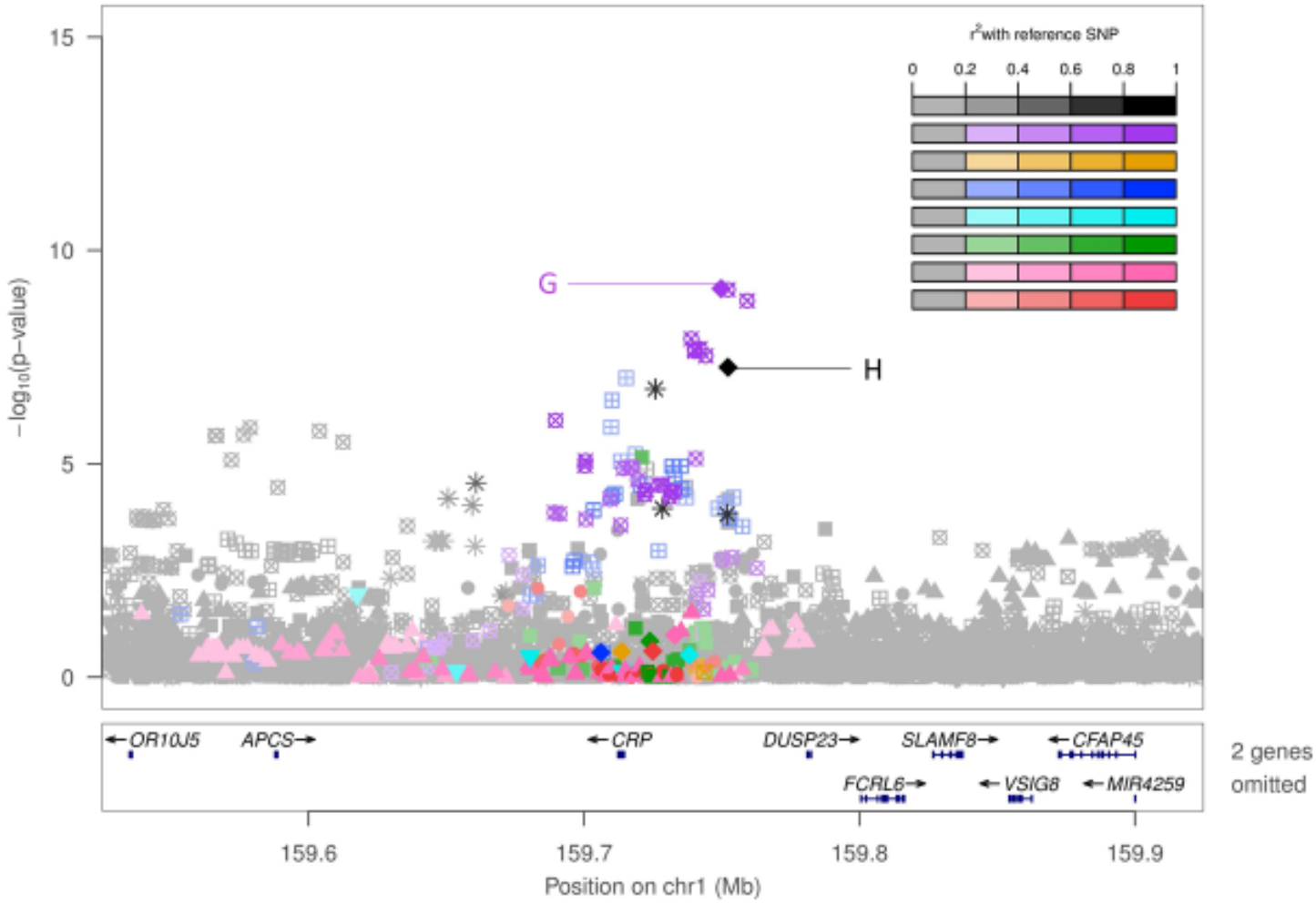

g. In ancestry pooled analysis, LocusZoom plot of association results conditioned on rs7551731, rs73024795, rs2211321, rs553202904, rs11265259, rs1800947, and rs12734907 (lead variant rs181704186).

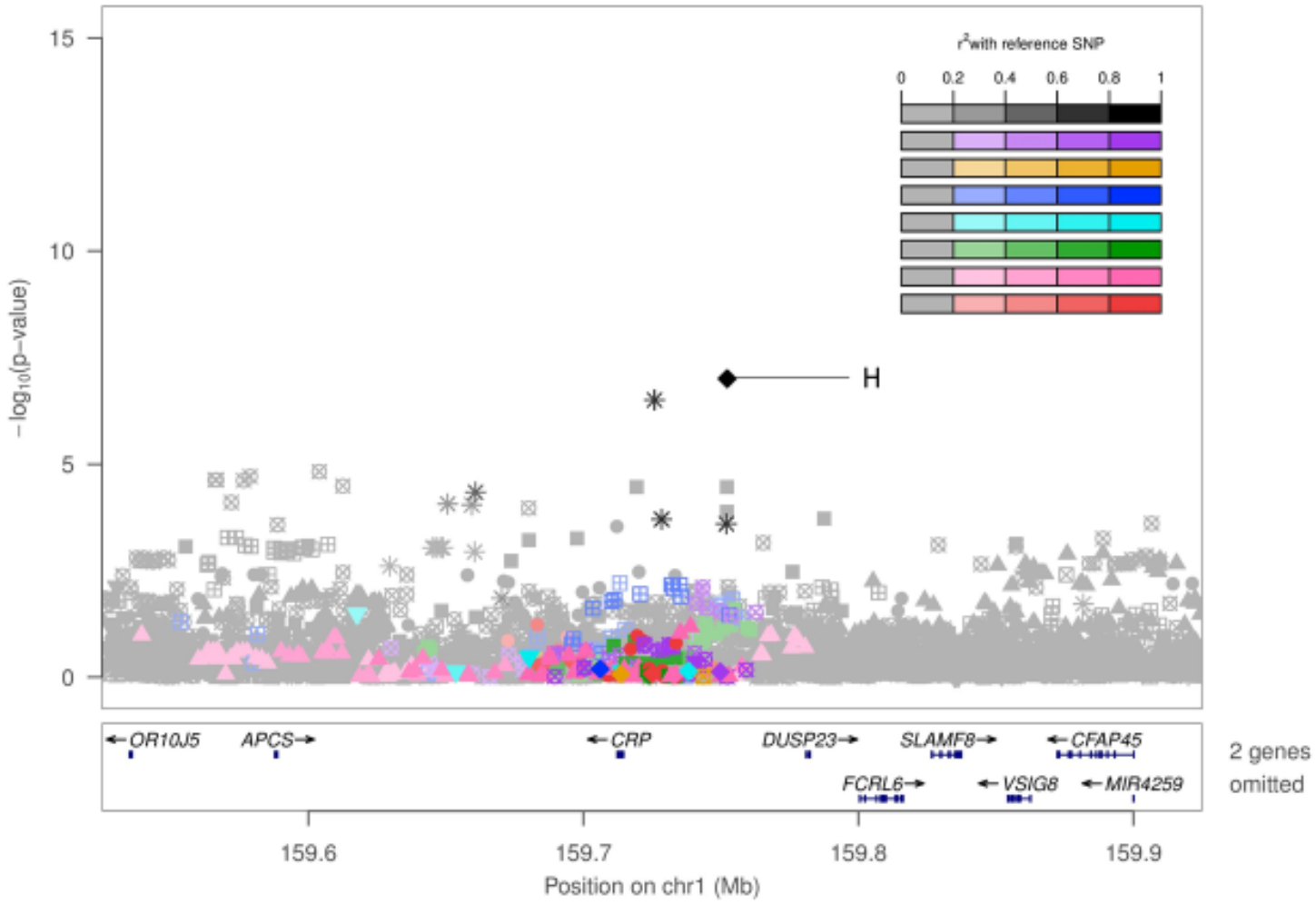

h. Ancestry pooled analysis conditioned on all previously known variants from GWAS and exome sequencing studies. Only signals E and H are labelled, as these are the only signals still reaching our locus-wide significance threshold (as listed in Table 1).

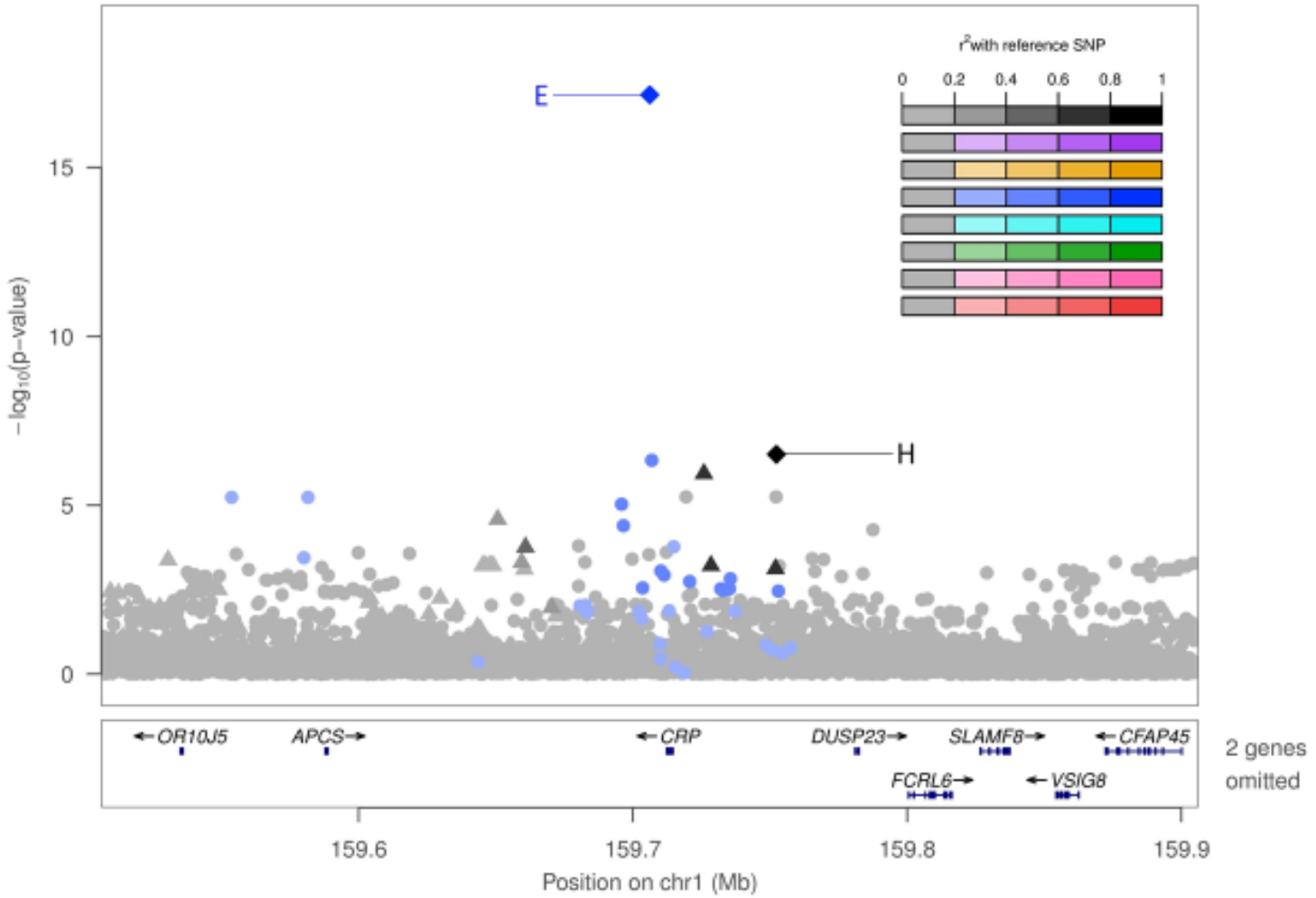

Figure S3: LocusZoom plots for sequential conditional analysis results at *CRP* locus, as well as plot of *CRP* locus adjusting for all previously identified *CRP* locus variants, with ancestry stratified LD reference panels.

a. In ancestry pooled analysis, LocusZoom plot of association results (lead variant rs7551731). Letters in this and subsequent figures correspond to the list of conditionally distinct signals in Table 2. All plots display -log10(p-value) versus genomic location for all distinct signals subsequent to ones conditioned on, using order from Table. The lead variant for each conditionally distinct signal is indicated with a diamond, with other variants in linkage disequilibrium r^2>0.2 indicated in the colors used for each letter label and displayed on the legend at right, each with a different shape (for example, variants in close linkage disequilibrium with signal B (rs73024795) are displayed as pink triangles). Linkage disequilibrium is calculated based on European American participants in TOPMed CRP analysis; association statistics are from pooled analysis.

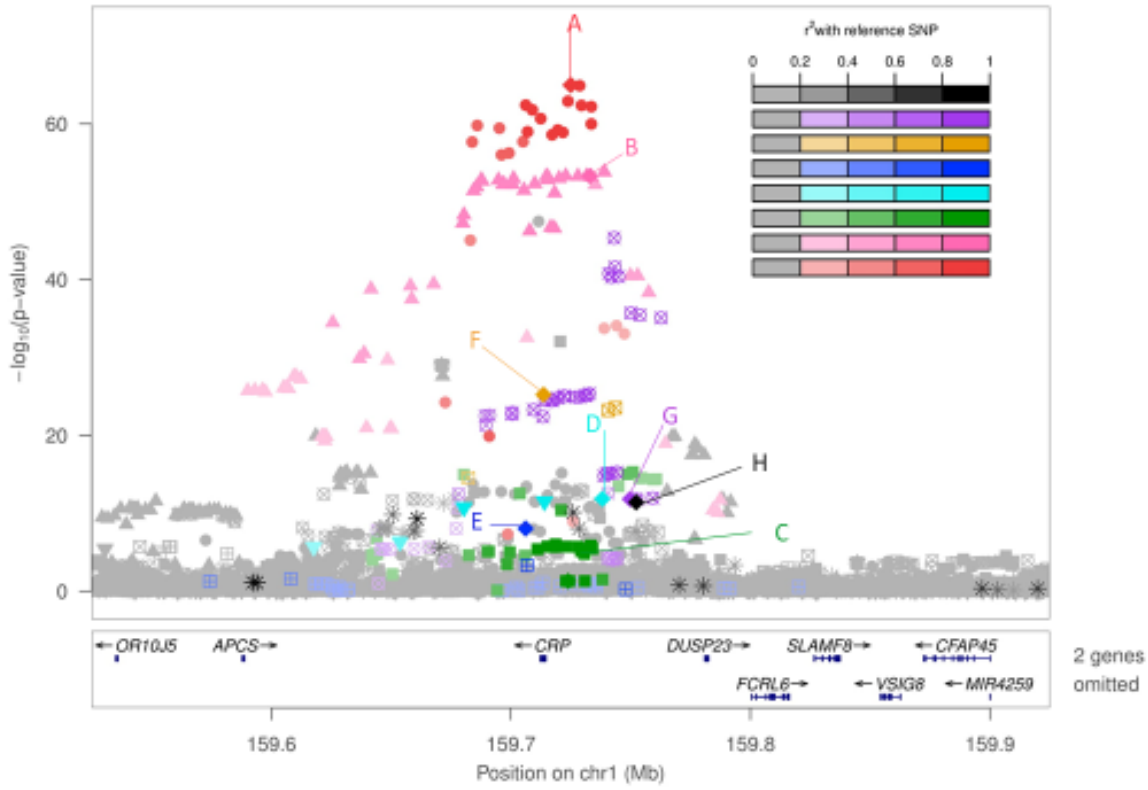

b. In ancestry pooled analysis, LocusZoom plot of association results conditioned on rs7551731 (lead variant rs73024795). Linkage disequilibrium is calculated based on European American participants in TOPMed CRP analysis; association statistics are from pooled analysis.

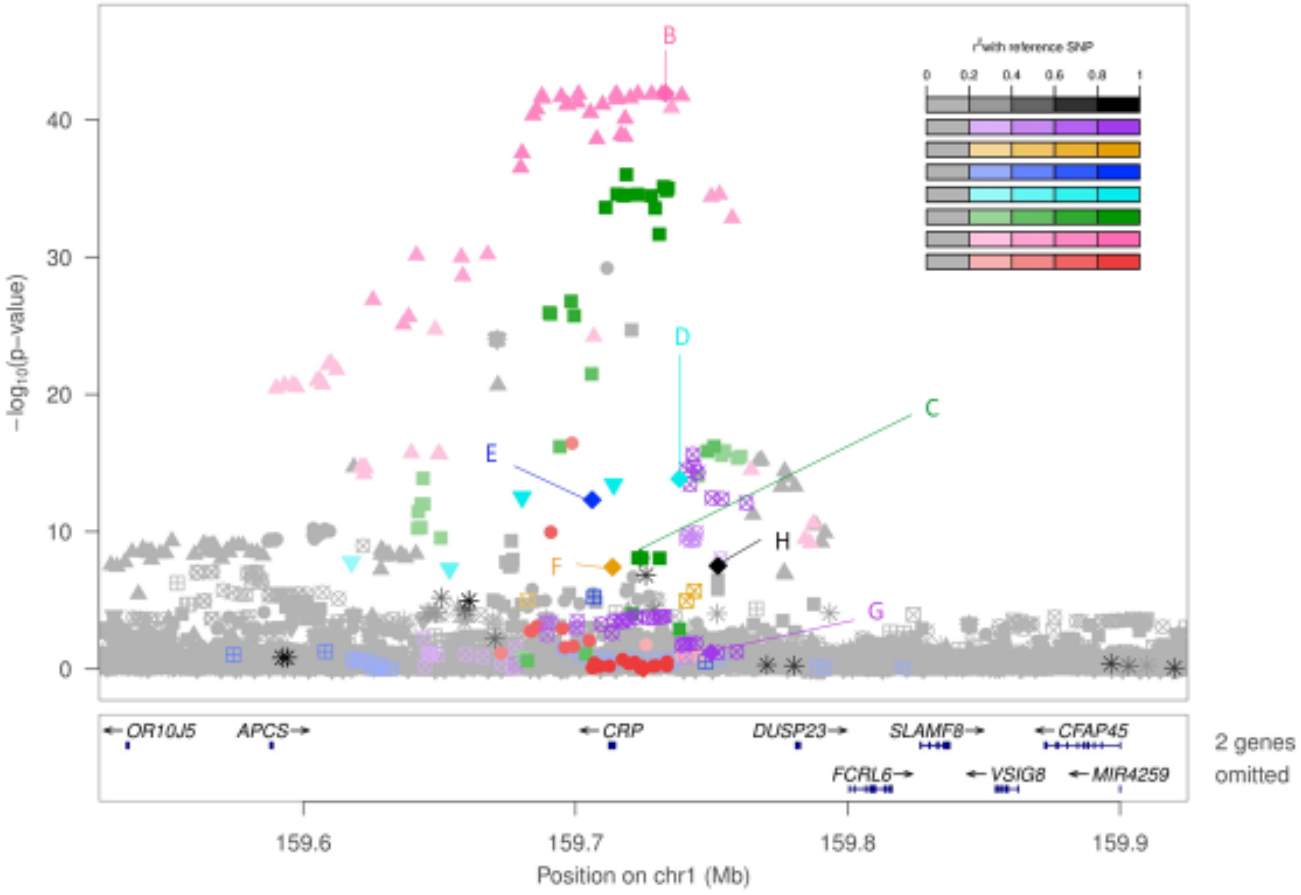

c. In ancestry pooled analysis, LocusZoom plot of association results conditioned on rs7551731 and rs73024795 (lead variant rs2211321). Linkage disequilibrium is calculated based on European American participants in TOPMed CRP analysis; association statistics are from pooled analysis.

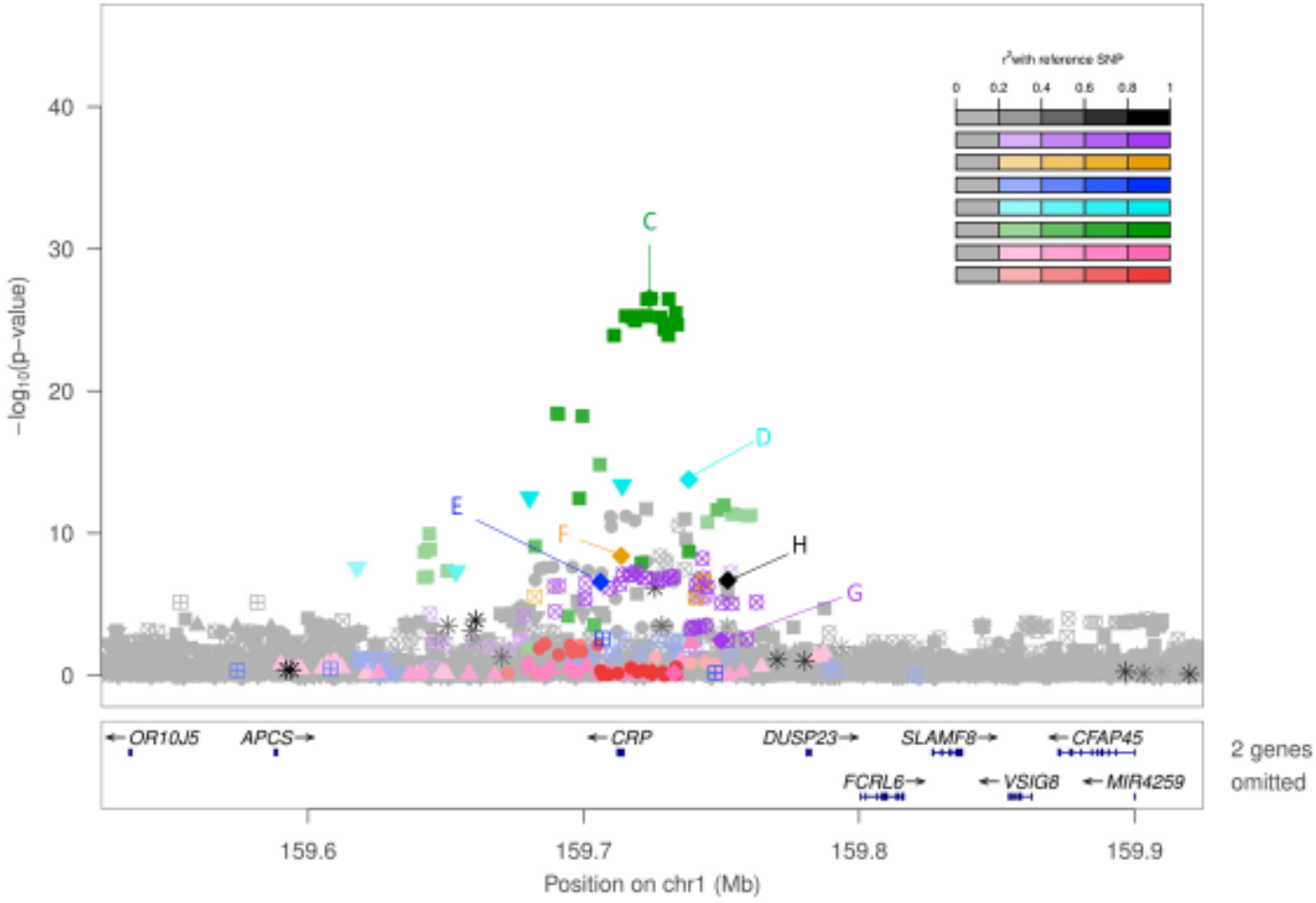

d. In ancestry pooled analysis, LocusZoom plot of association results conditioned on rs7551731, rs73024795, and rs2211321 (lead variant rs553202904). Linkage disequilibrium is calculated based on European American participants in TOPMed CRP analysis; association statistics are from pooled analysis.

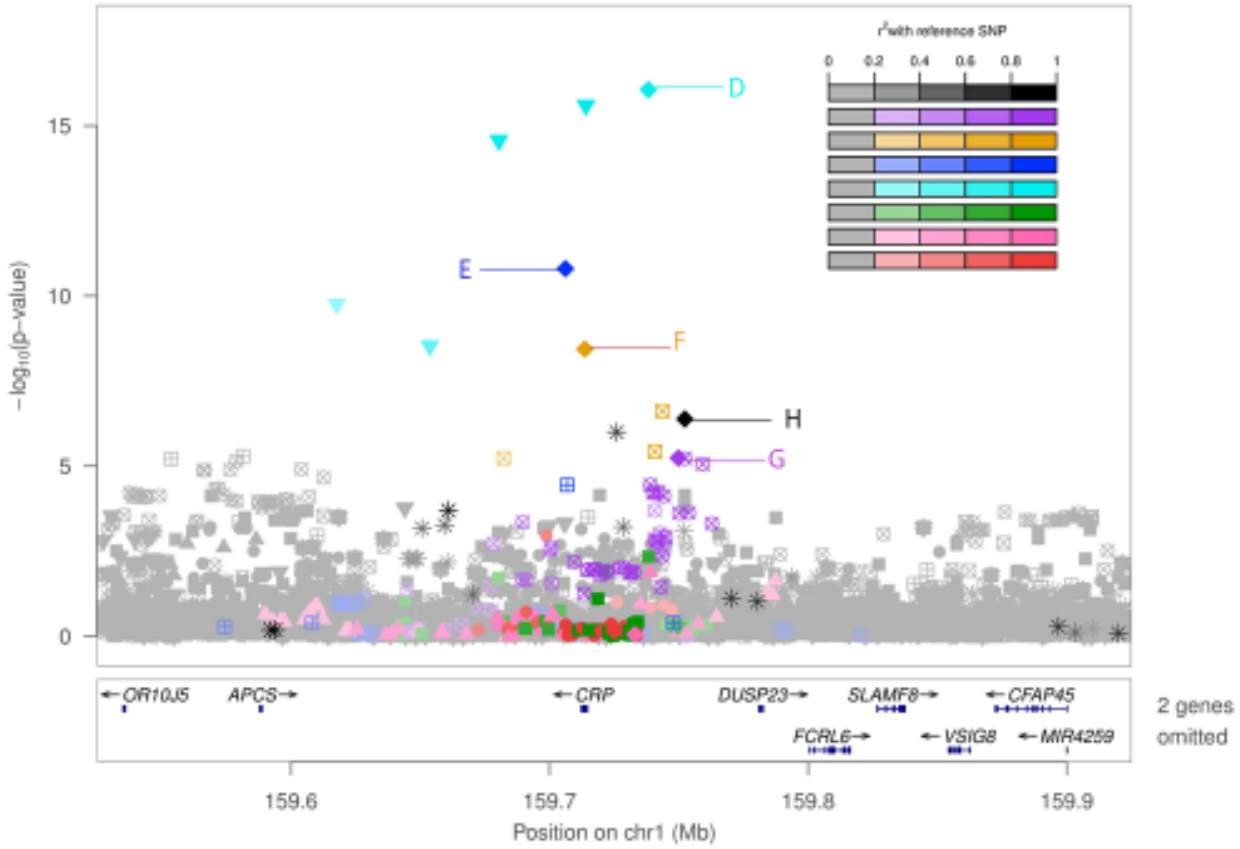

e. In ancestry pooled analysis, LocusZoom plot of association results conditioned on rs7551731, rs73024795, rs2211321, and rs553202904 (lead variant rs11265259). Linkage disequilibrium is calculated based on European American participants in TOPMed CRP analysis; association statistics are from pooled analysis.

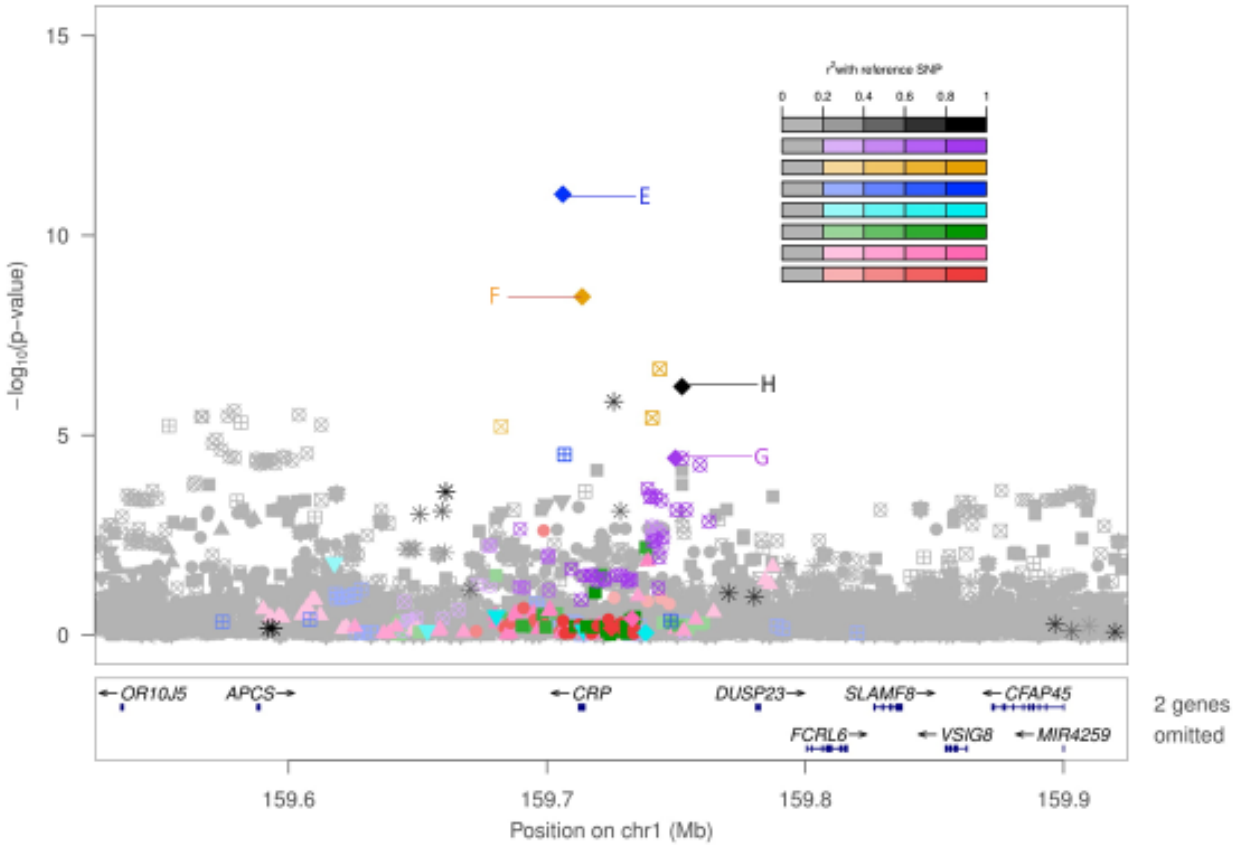

f. In ancestry pooled analysis, LocusZoom plot of association results conditioned on rs7551731, rs73024795, rs2211321, rs553202904, and rs11265259 (lead variant rs1800947). Linkage disequilibrium is calculated based on European American participants in TOPMed CRP analysis; association statistics are from pooled analysis.

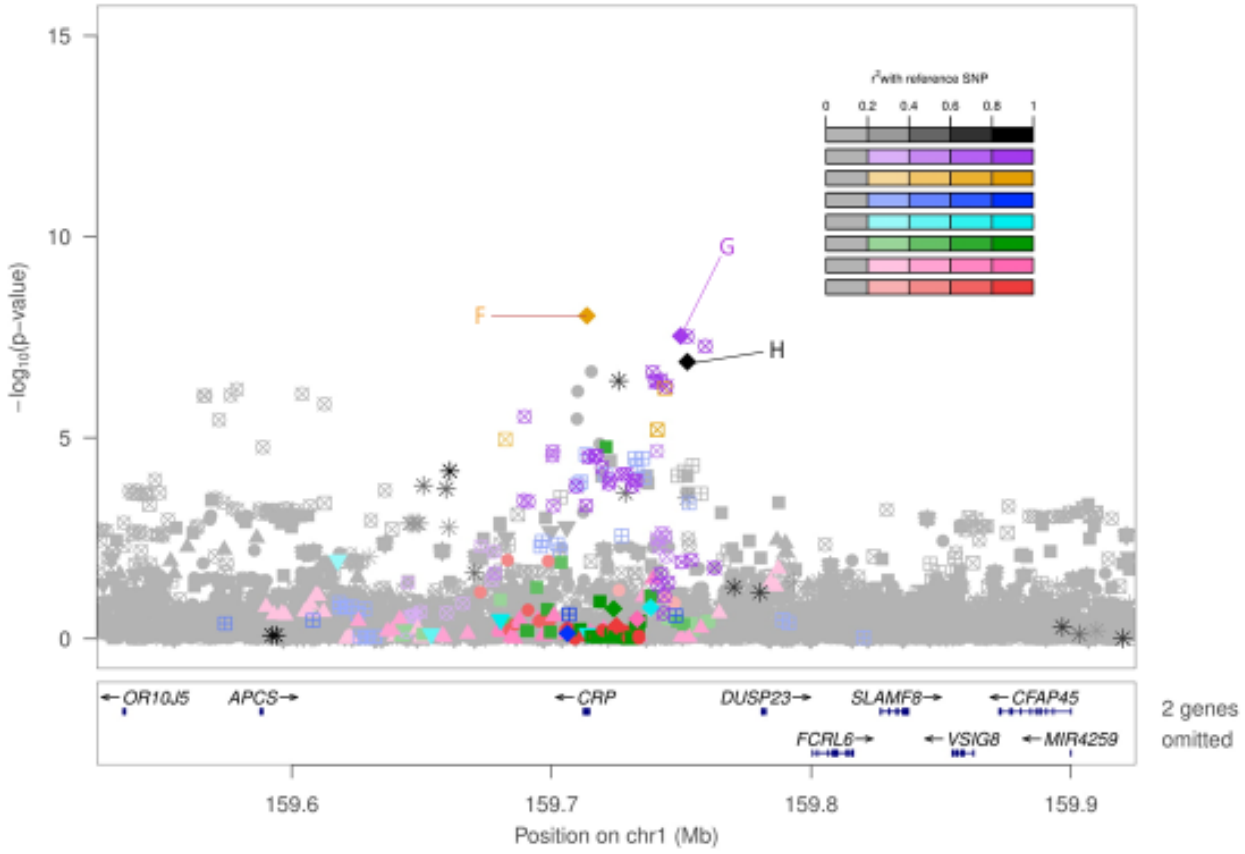

g. In ancestry pooled analysis, LocusZoom plot of association results conditioned on rs7551731, rs73024795, rs2211321, rs553202904, rs11265259, and rs1800947 (lead variant rs12734907). Linkage disequilibrium is calculated based on European American participants in TOPMed CRP analysis.

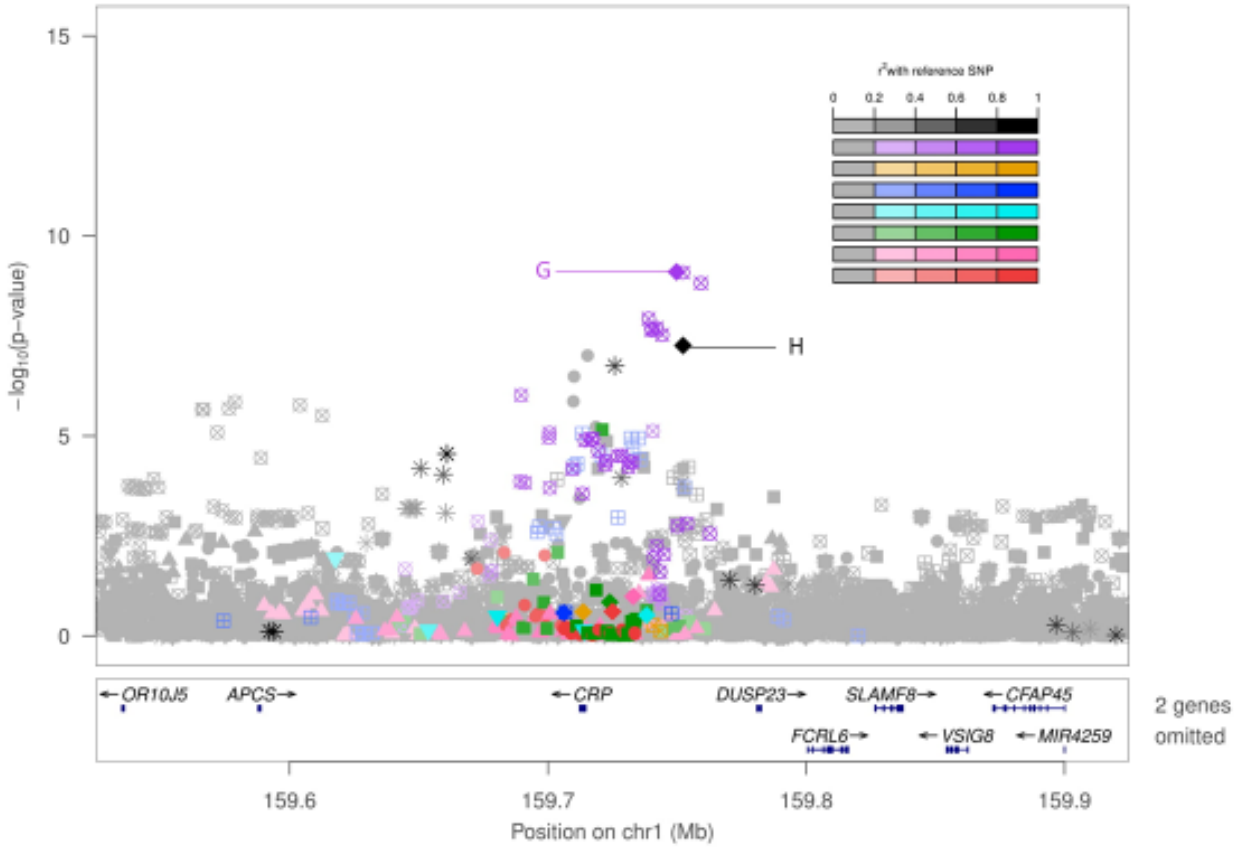

h. In ancestry pooled analysis, LocusZoom plot of association results conditioned on rs7551731, rs73024795, rs2211321, rs553202904, rs11265259, rs1800947, and rs12734907 (lead variant rs181704186). Linkage disequilibrium is calculated based on European American participants in TOPMed CRP analysis; association statistics are from pooled analysis.

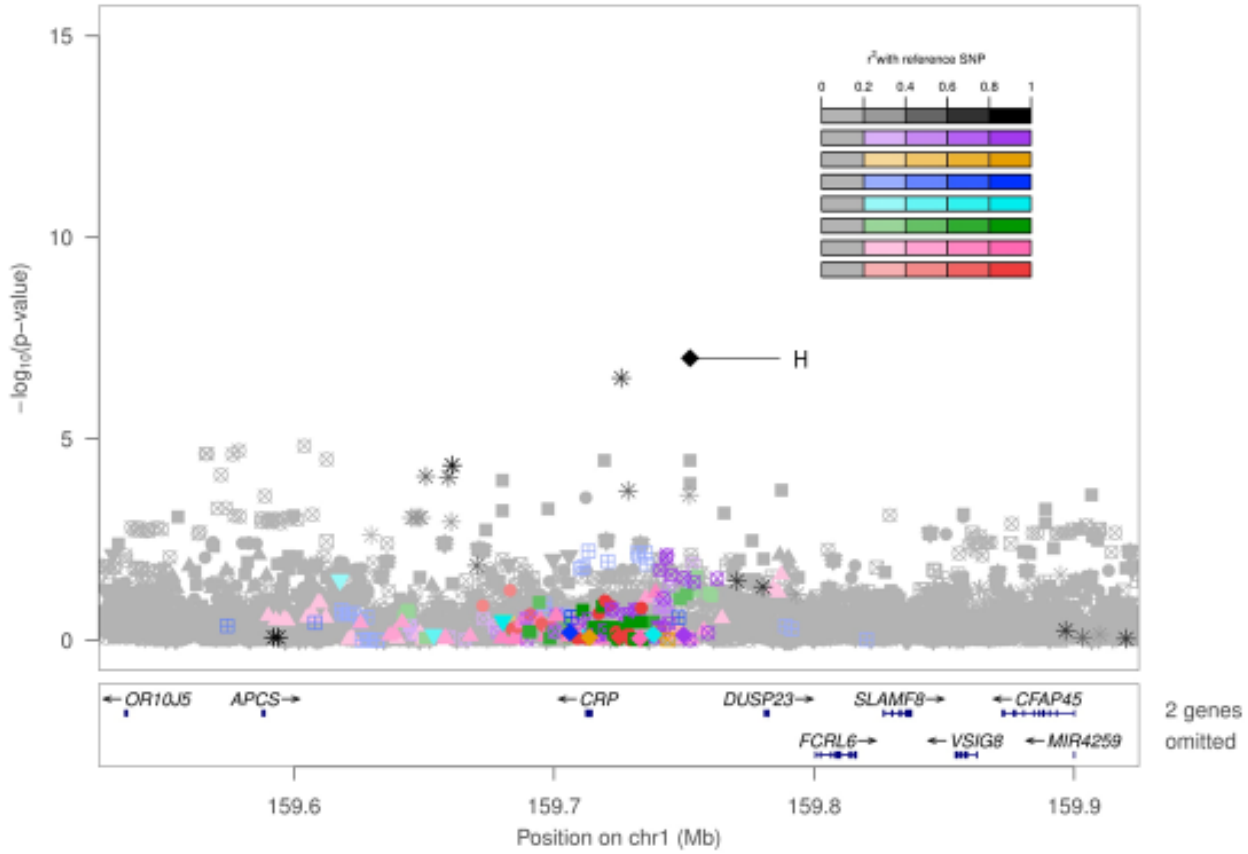

i. Ancestry pooled analysis conditioned on all previously known variants from GWAS and exome sequencing studies. Only signals E and H are labelled, as these are the only signals still reaching our locus-wide significance threshold (as listed in Table 1). Linkage disequilibrium is calculated based on European American participants in TOPMed CRP analysis; association statistics are from pooled analysis.

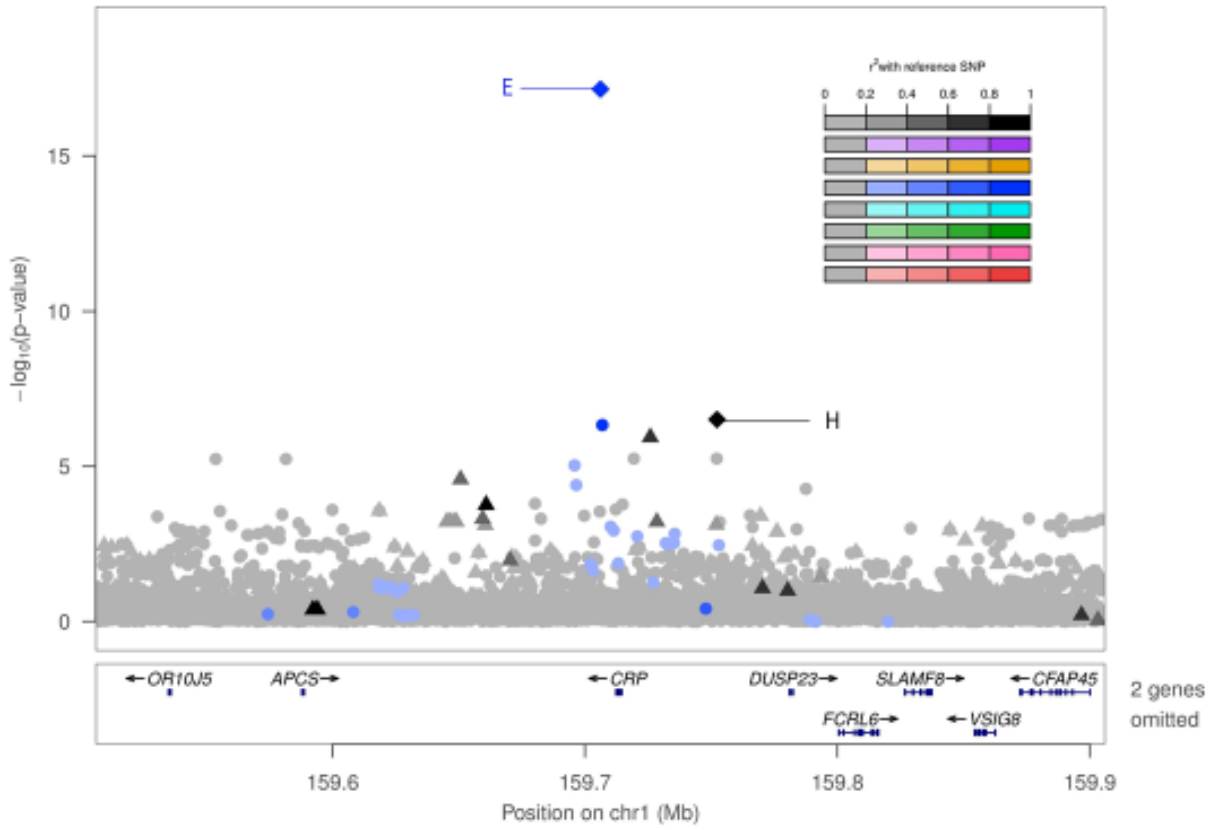

j. In ancestry pooled analysis, LocusZoom plot of association results (lead variant rs7551731). Linkage disequilibrium is calculated based on African American participants in TOPMed CRP analysis; association statistics are from pooled analysis.

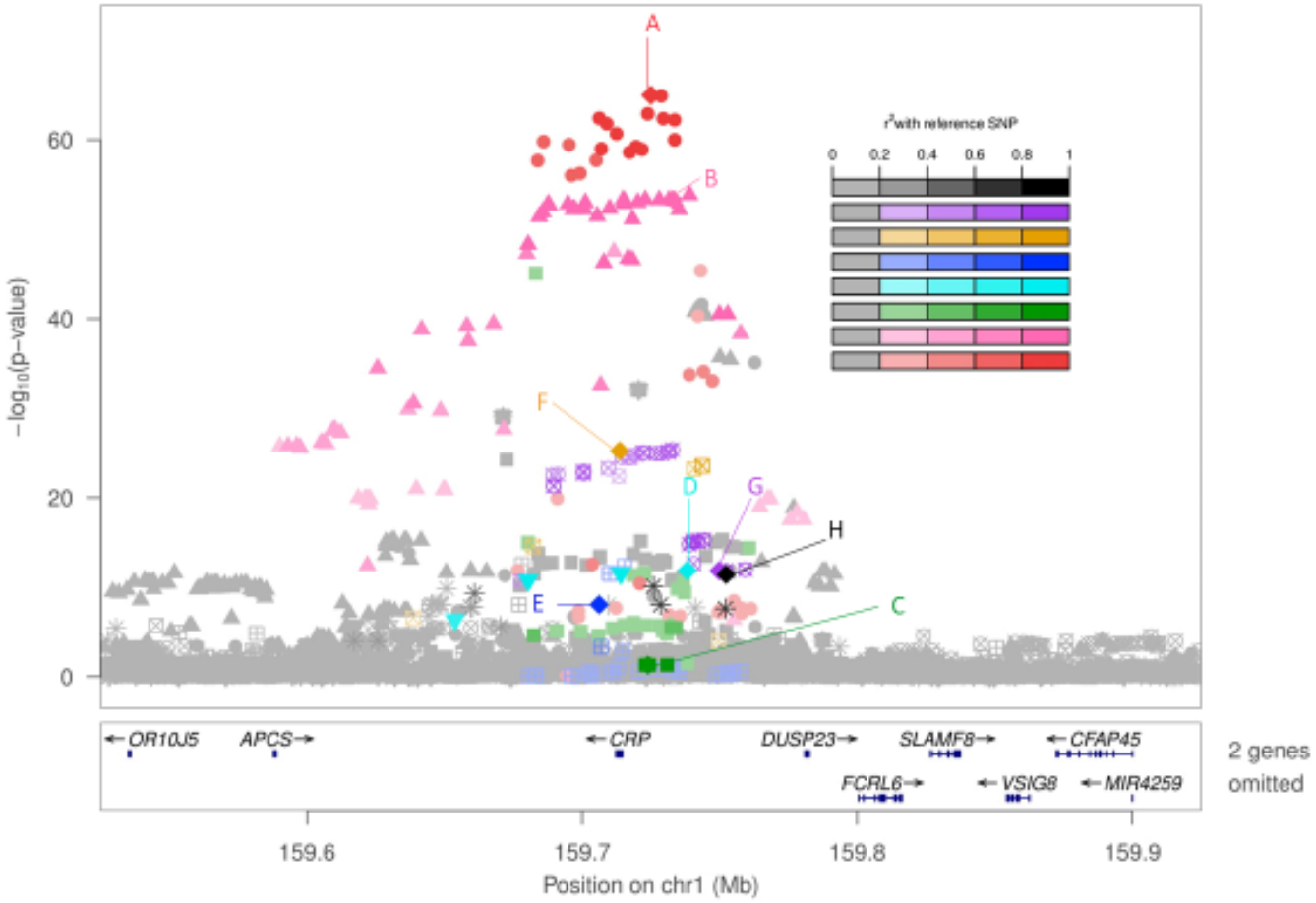

k. In ancestry pooled analysis, LocusZoom plot of association results conditioned on rs7551731 (lead variant rs73024795). Linkage disequilibrium is calculated based on African American participants in TOPMed CRP analysis; association statistics are from pooled analysis.

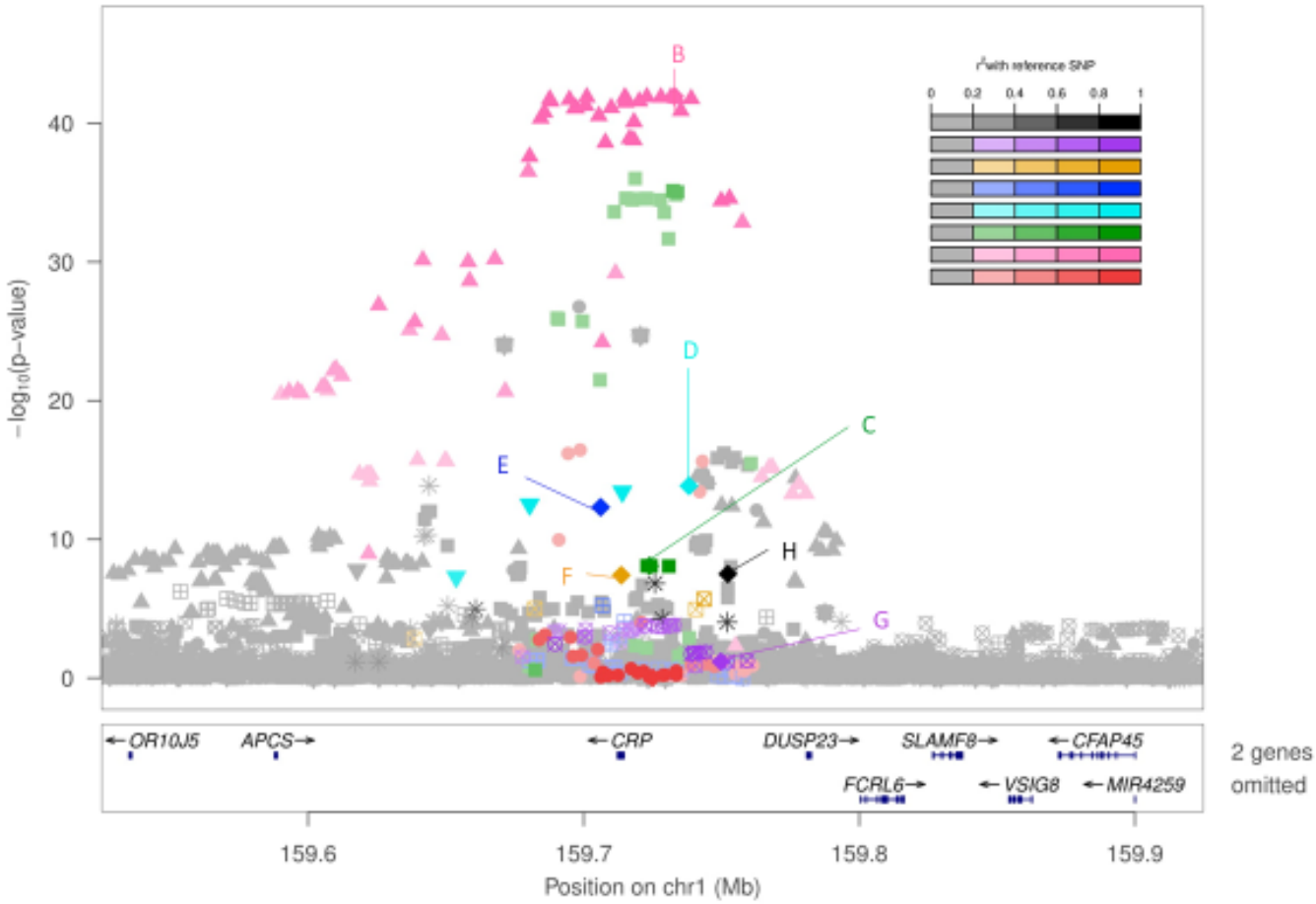

I. In ancestry pooled analysis, LocusZoom plot of association results conditioned on rs7551731 and rs73024795 (lead variant rs2211321). Linkage disequilibrium is calculated based on African American participants in TOPMed CRP analysis; association statistics are from pooled analysis.

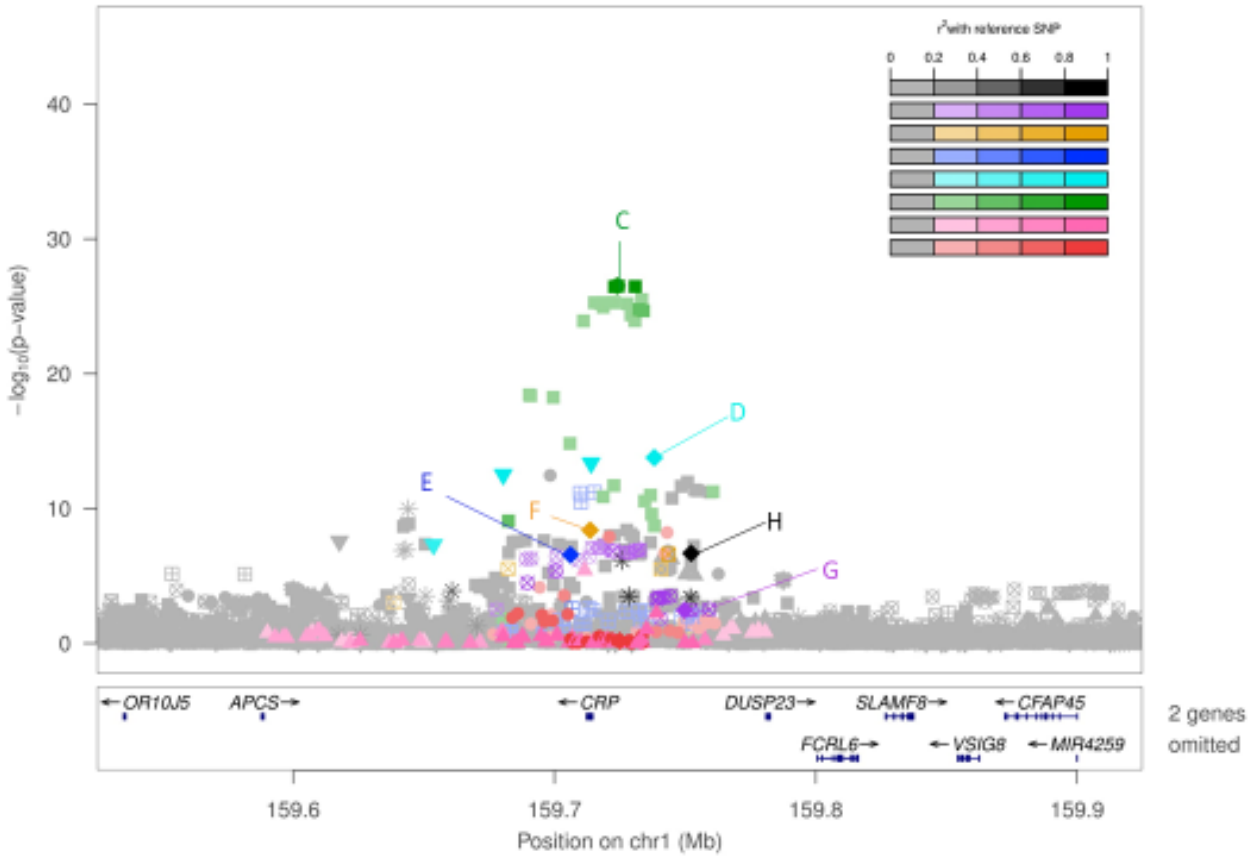

m. In ancestry pooled analysis, LocusZoom plot of association results conditioned on rs7551731, rs73024795, and rs2211321 (lead variant rs553202904). Linkage disequilibrium is calculated based on African American participants in TOPMed CRP analysis; association statistics are from pooled analysis.

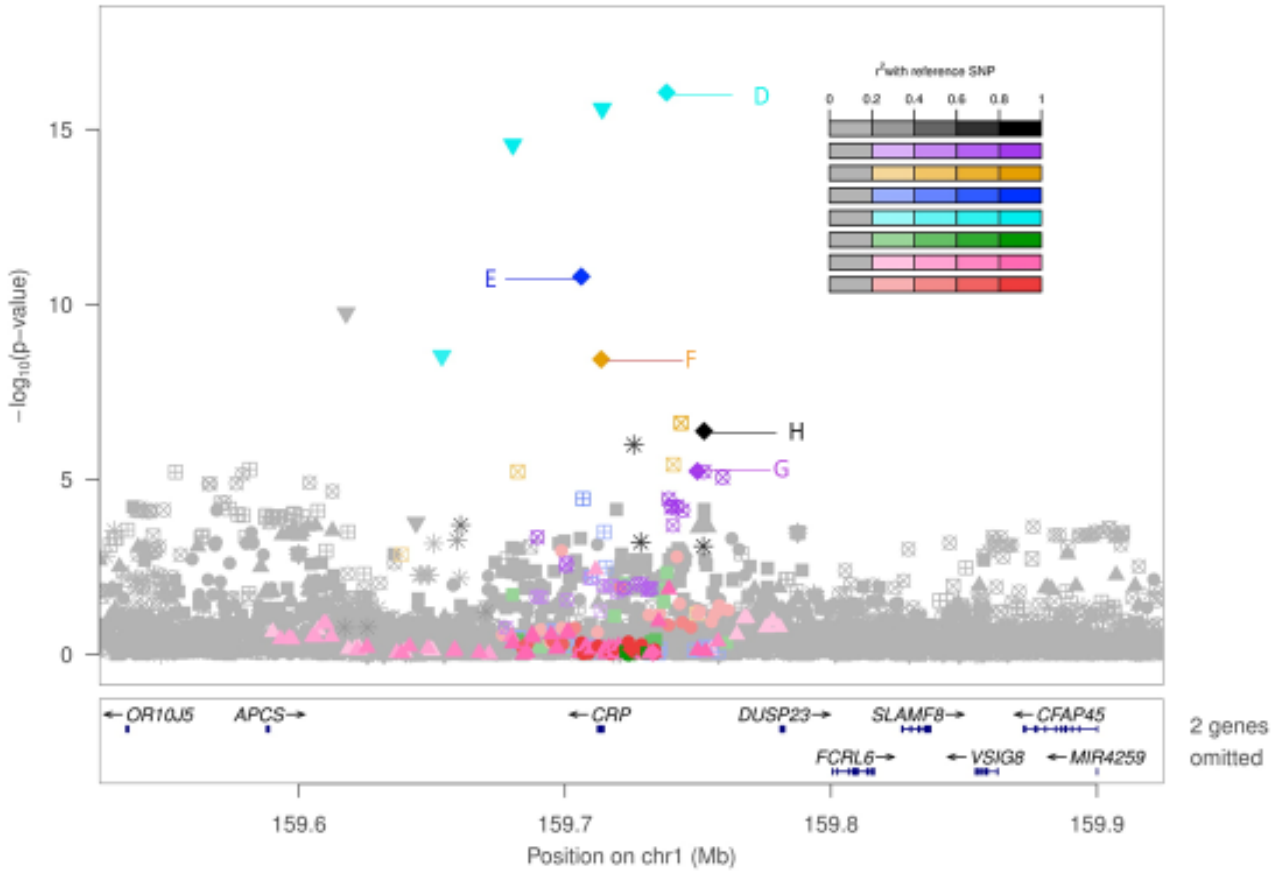

n. In ancestry pooled analysis, LocusZoom plot of association results conditioned on rs7551731, rs73024795, rs2211321, and rs553202904 (lead variant rs11265259). Linkage disequilibrium is calculated based on African American participants in TOPMed CRP analysis; association statistics are from pooled analysis.

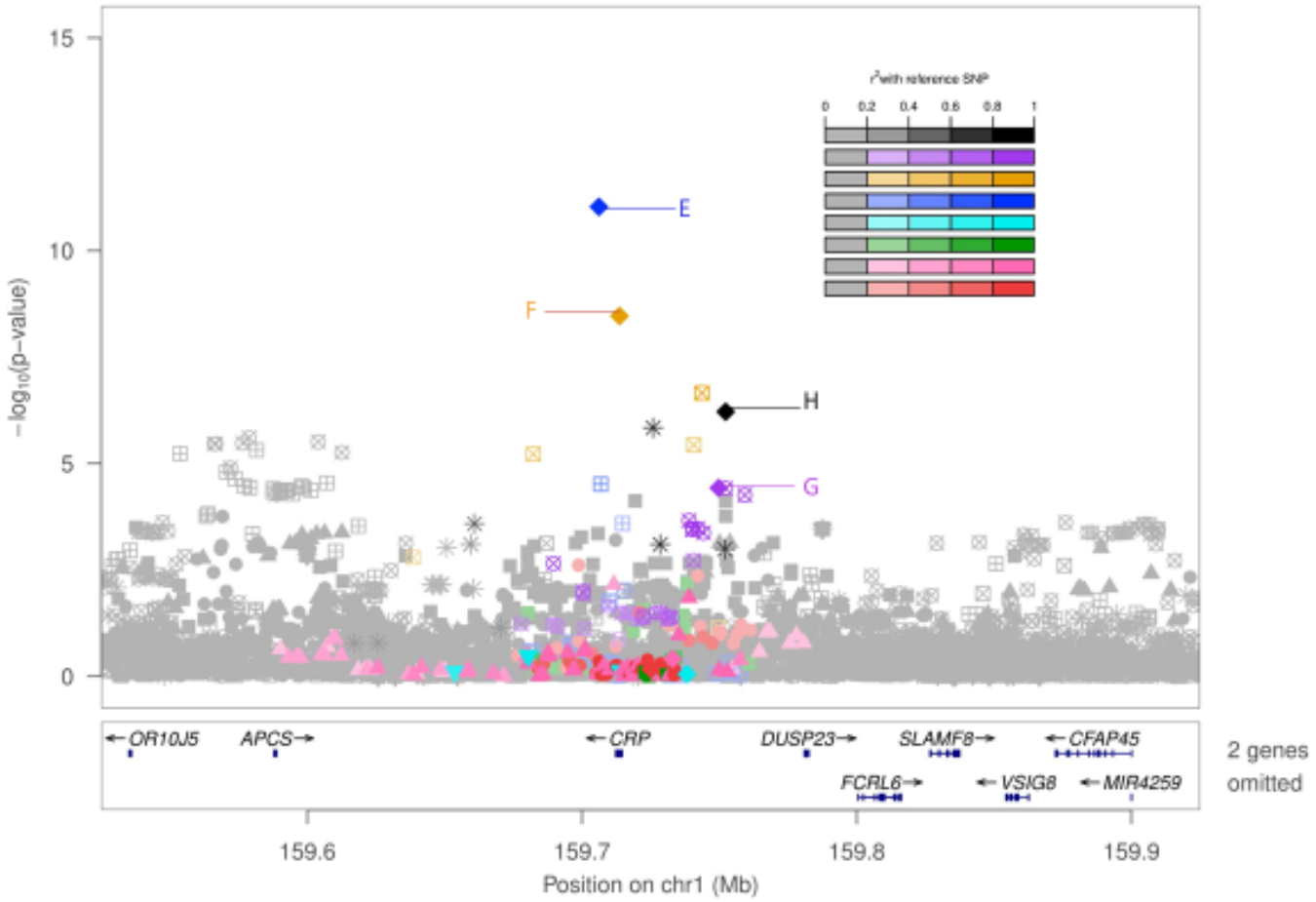

o. In ancestry pooled analysis, LocusZoom plot of association results conditioned on rs7551731, rs73024795, rs2211321, rs553202904, and rs11265259 (lead variant rs1800947). Linkage disequilibrium is calculated based on African American participants in TOPMed CRP analysis; association statistics are from pooled analysis.

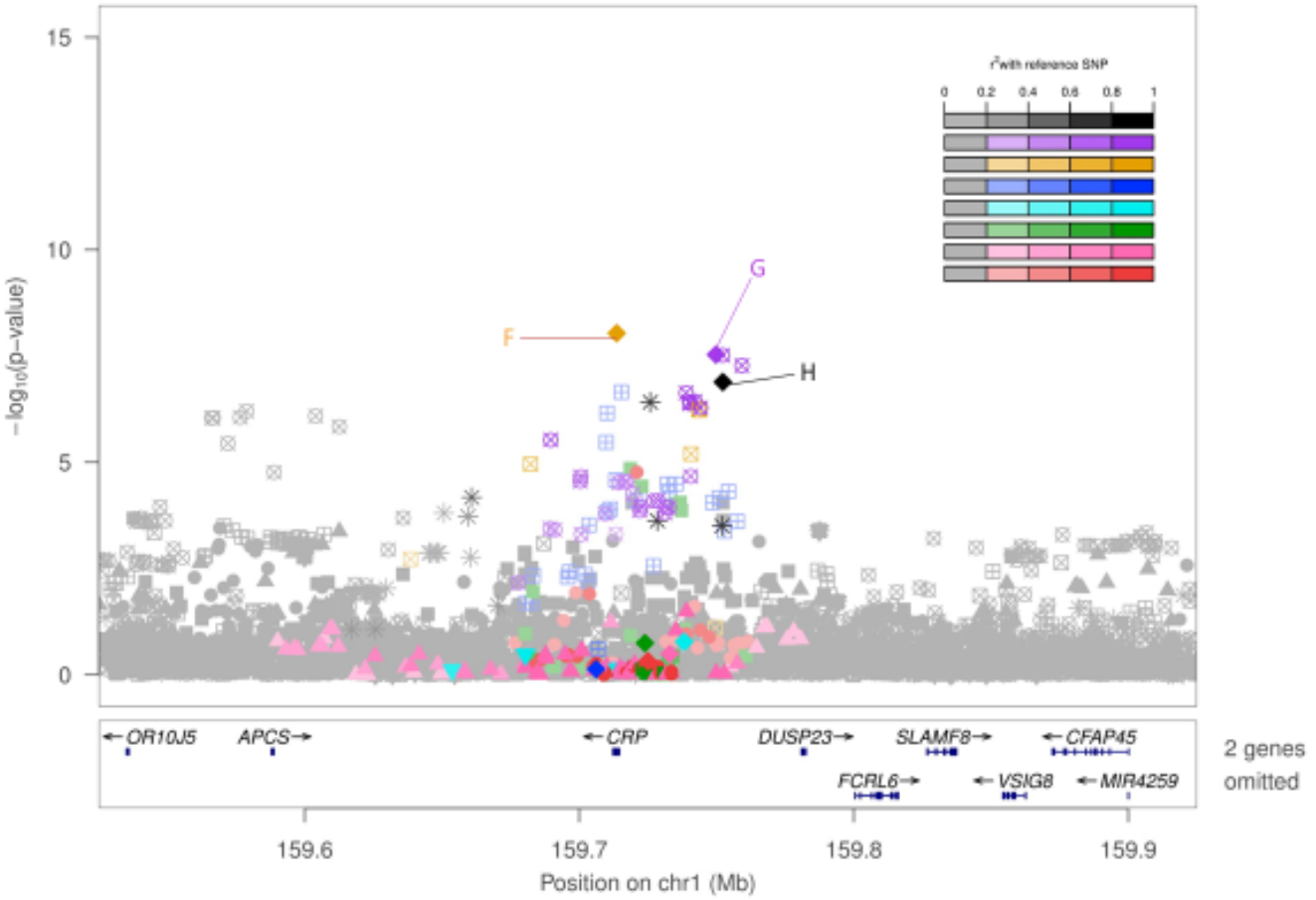

p. In ancestry pooled analysis, LocusZoom plot of association results conditioned on rs7551731, rs73024795, rs2211321, rs553202904, rs11265259, and rs1800947 (lead variant rs12734907). Linkage disequilibrium is calculated based on African American participants in TOPMed CRP analysis.

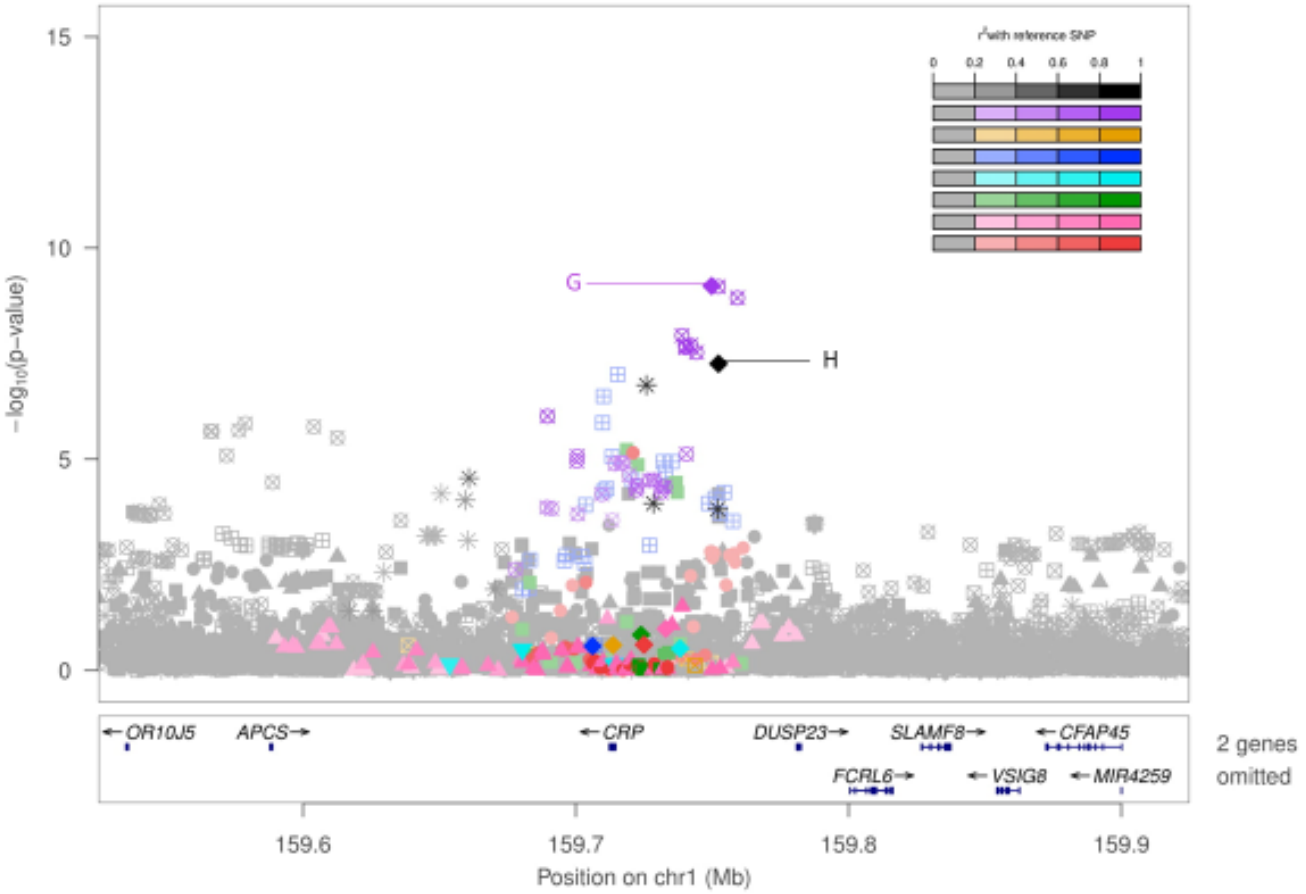

q. In ancestry pooled analysis, LocusZoom plot of association results conditioned on rs7551731, rs73024795, rs2211321, rs553202904, rs11265259, rs1800947, and rs12734907 (lead variant rs181704186). Linkage disequilibrium is calculated based on African American participants in TOPMed CRP analysis; association statistics are from pooled analysis.

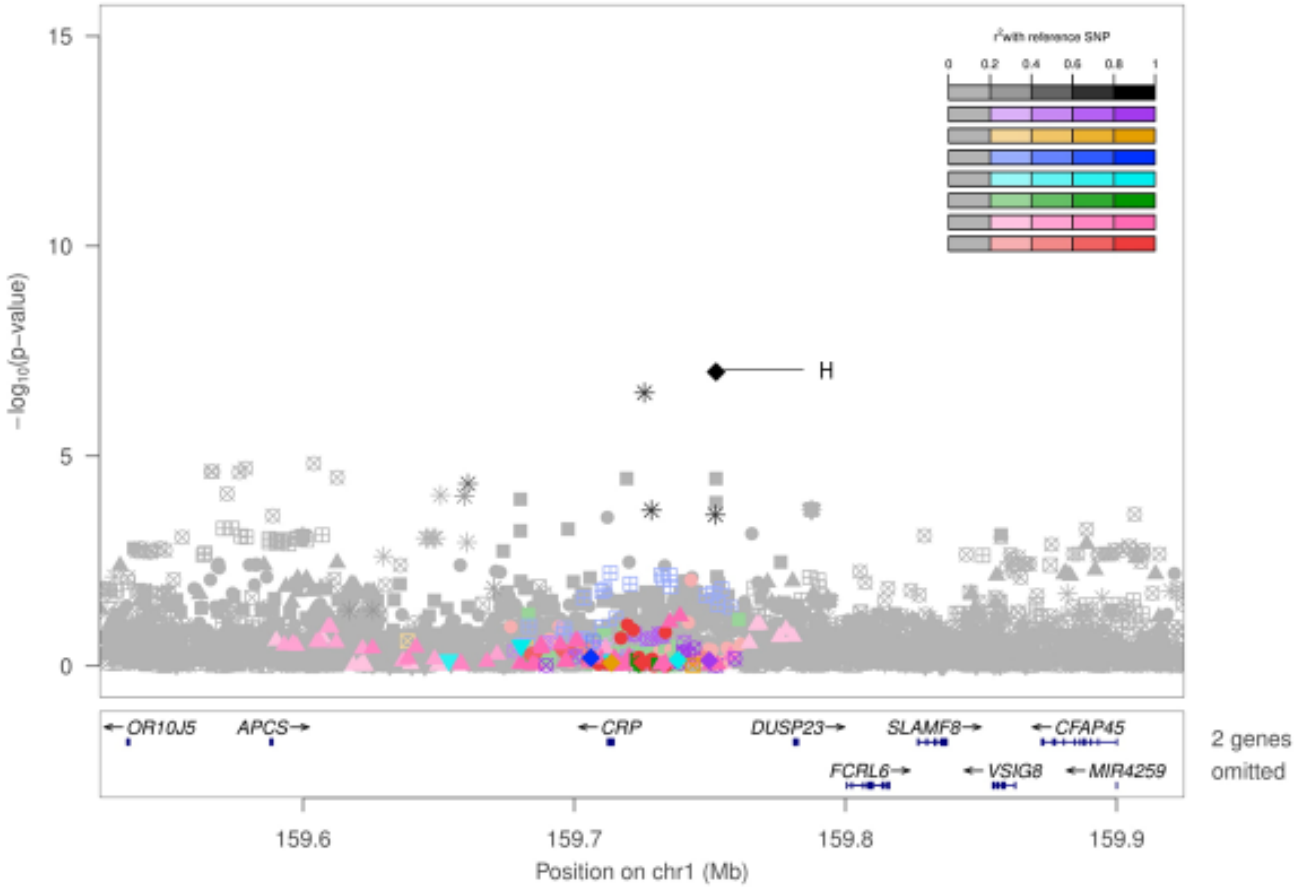

r. Ancestry pooled analysis conditioned on all previously known variants from GWAS and exome sequencing studies. Only signals E and H are labelled, as these are the only signals still reaching our locus-wide significance threshold (as listed in Table 1). Linkage disequilibrium is calculated based on African American participants in TOPMed CRP analysis; association statistics are from pooled analysis.

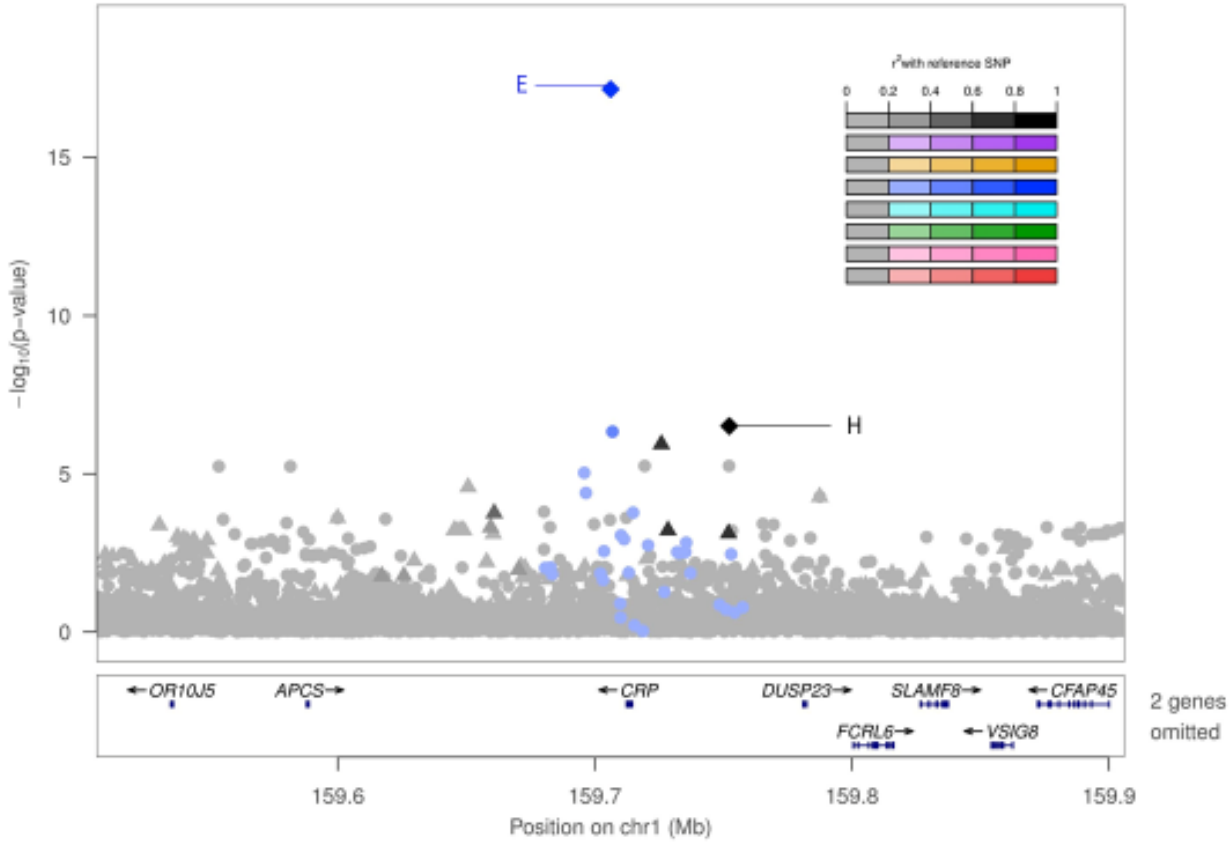

Figure S4: **Functional annotation information for rs11265259.** Genome browser plot for rs11265259, displaying UCSC genes, chromHMM annotation in adult liver (yellow=enhancer, green=weak transcription, red=transcription start site) from RoadMap Epigenomics, H3K4me1 signal from adult liver, 100 vertebrates basewise conservation by PhyloP, and transcription factor ChIP-seq clusters from ENCODE (161 factor version, motifs highlighted in green, proportion cell types detected/ total number of cell types assayed displayed). Unlike in the plot for rs181704186, we did not display GeneHancer due to lack of any relevant signals. No other variants have linkage disequilibrium r2 ≥ 0.8 with lead variant rs11265259.

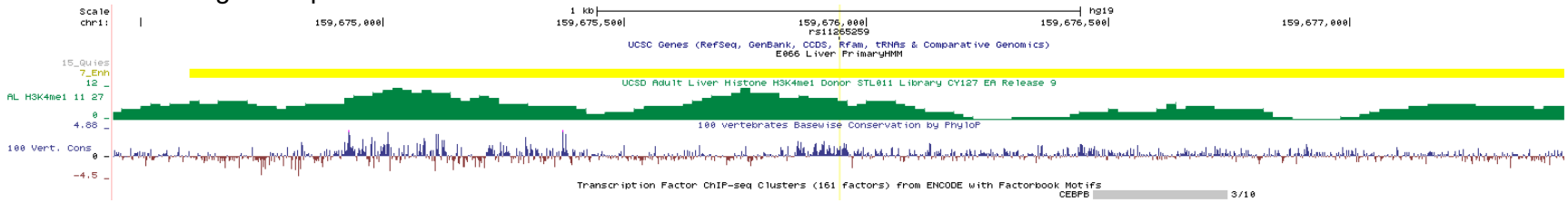

Figure S5: Additional Information for Functional Assays.

a. Additional luciferase assay for rs181704186. Blue lines indicate the groups compared for each listed p-value.

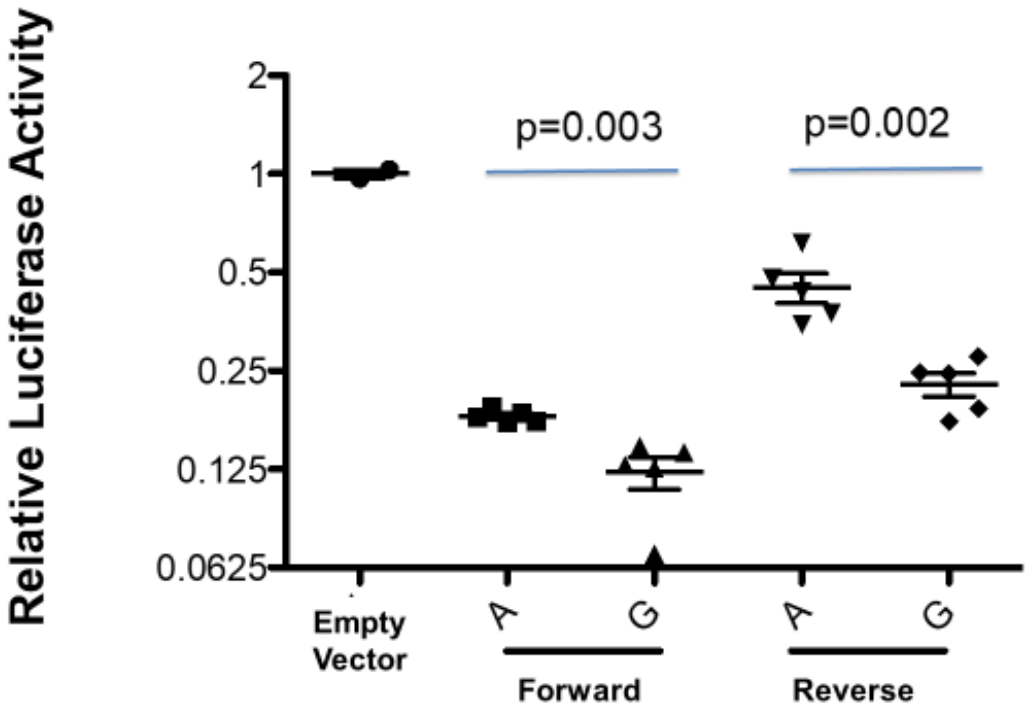

b. Full EMSA from main text Figure 2. NE, nuclear extract.

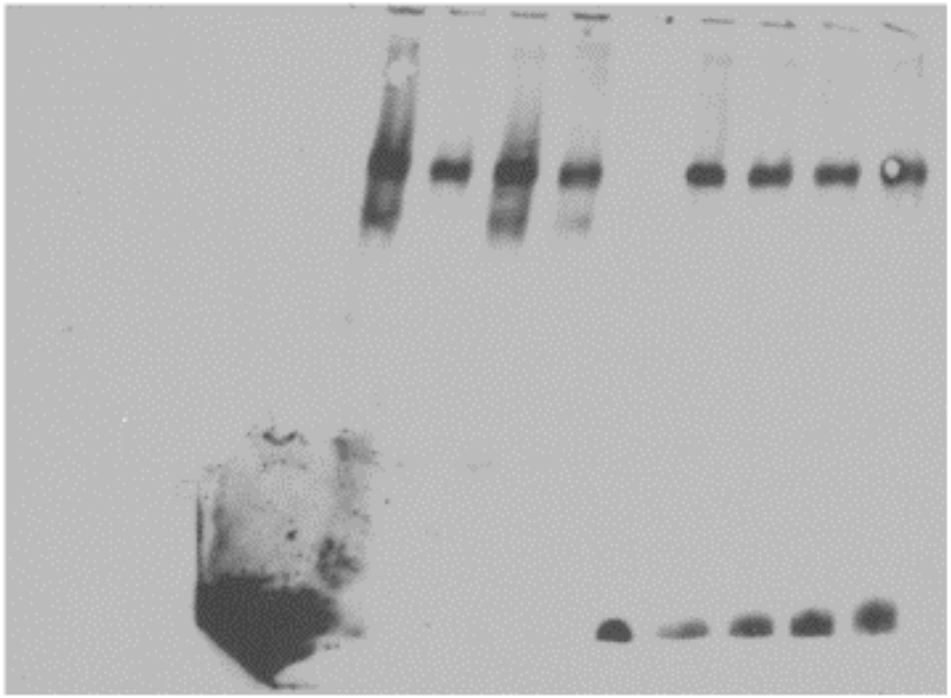

Lane	1	2	3	4	5	6	7	8	9	10
Labeled probe	A	A	A	A	A	G	G	G	G	G
HepG2 NE	-	+	+	+	+	-	+	+	+	+
Unlabeled competition (40x)	-	-	A	G	-	-	-	A	G	-
CEBPB antibody	-	-	-	-	+	-	-	-	-	+

c. Additional replicate of EMSA for rs181704186. EMSA with biotin-labeled probes containing the A or G allele of rs181704186 shows an allele-specific band (arrow; lane 2 versus 6) that is competed away by 40-fold excess of unlabeled probe containing the A allele (lane 3), but unaffected by a 40-fold excess of probe containing the G allele (lane 4). NE, nuclear extract.

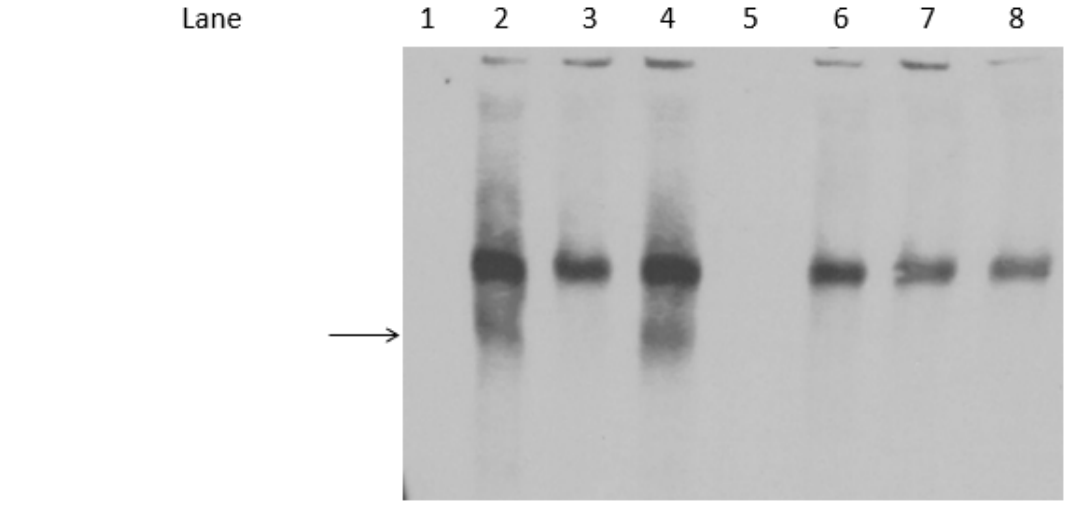

d. Full EMSA from Figure S4c.

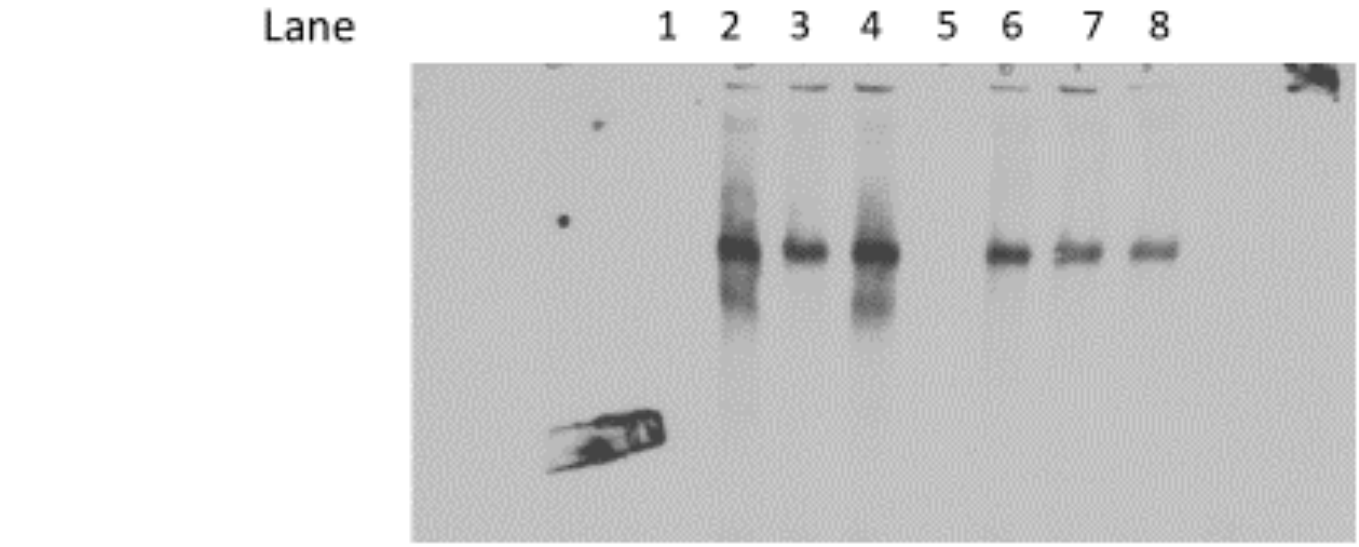

Table S1: Cohort demographic characteristics and C-reactive protein assays.

Study	N	Mean (SD) Age	% female	Mean (SD) C-reactive Protein	Self-Reported Ancestry	Case/control status (if used for sample selection)	Assay
Atherosclerosis Risk in Communities (ARIC)	2,433	63.7 (5.6)	51.1%	4.3 (6.2)	95.9% EA, 4.1% AA	Case 5.5% (VTE or atrial fibrillation), control 94.5%	BNII analyzer (Siemens Healthcare Diagnostics, Deerfield, Illinois)[1]
Cleveland Family Study (CFS)	570	42.3 (18.7)	56.0%	4.4 (6.1)	42.1% EA, 54.9% AA, 3.0% Multiple	NA	Dade Behring BNII nephelometer
Framingham Heart Study (FHS)	3,151	53.0 (14.3)	53.5%	3.5 (5.1)	EA	NA	Dade Behring BN 100 High Sensitivity CRP Agent, Dade Behring CardioPhase hsCRP, Roche cobas c501 CRP High Sensitivity Assay
Genetic Epidemiology of COPD (COPDGene)	504	63.6 (8.7)	51.0%	4.8 (5.8)	EA	NA	Myriad RBM custom multiplex[2]
Genetic Studies of Atherosclerosis Risk (GeneSTAR)	1,525	43.0 (11.9)	60.3%	2.9 (3.1)	55.6% EA, 44.4% AA	NA	Dako and E80C
Jackson Heart Study (JHS)	3,035	55.5 (12.8)	61.9%	5.0 (7.3)	AA	NA	Immunoturbidimetric CRP-Latex assay (Kamiya Biomedical Company, Seattle, WA) using a Hitachi 911 analyzer (Roche Diagnostics, Indianapolis, IN)[3]
Multi-Ethnic Study of Atherosclerosis (MESA) and MESA Family	4,289	61.1 (9.8)	51.5%	3.5 (4.9)	38.7% EA, 27.2% AA, 21.5% HL, 12.6% AS	NA	BNII nephelometer (Dade-Behring)[4]

Old Order Amish	988	49.4 (16.1)	50.1%	2.0 (3.4)	EA	NA	Nephelometry
Women's Health Initiative (WHI)	6,784	67.2 (6.7)	100.0%	4.9 (6.3)	18.5% AA, 78.7% EA, 3.9% HL, 0.7% AS 0.7 AI/AN, 0.2% Other	Case 47.1% (stroke and VTE), control 52.9%	Multiple assays, including BNII Nephlometer, DiaSorin, hs-immunotechnique - Behring analyzer (Denka Seiken; Niigata, Japan), Immulite Analyzer, a Roche Modular P Chemistryanalyzer, SPQ High Sensitivity ReagentHitachi Analyzer

Note that some individuals identify both as of African American or European American ancestry and as Hispanic/Latino.
Abbreviations: EA, European American; AA, African American; HL, Hispanic/Latino; AS, East Asian; AI/AN American Indians/Alaska Natives; VTE, venous thromboembolism; SD, standard deviation; NA, not applicable

Table S2a: Lead variants and number of distinct signals in European American specific association analysis

Locus	Lead Variant	Annotation	P-value	Beta	Effect Allele Frequency	Effect Allele	Number of distinct signals	Sequential Conditioning Lead Variants
LEPR	rs6588153	intronic	6.5E-16	-0.10	0.37	A	1	
IL6R	rs61812598	intronic	1.8E-07	-0.06	0.40	A	1	
CRP	rs2211320	intergenic	7.7E-39	-0.16	0.32	A	4	rs4425982, rs553202904, rs1800947
NLRP3	rs10157379	intronic	1.1E-05	0.05	0.62	T	0	
GCKR	rs1260326	missense, p.Leu446Pro (*GCKR*)	1.2E-12	-0.09	0.58	C	1	
IL1F10	rs28648961	intergenic	1.1E-07	0.07	0.40	A	1	
HNF1A	rs11065384	intronic	1.0E-25	0.13	0.67	C	1	
APOE	rs429358	missense, p.Cys130Arg (*APOE4*)	1.6E-42	-0.24	0.13	C	1	

Analysis was performed at 8 loci (500 kb ± genome-wide significant variants) identified in the pooled ancestry analysis. We used the same locus-wide thresholds as pooled ancestry analysis in Table 1.

Table S2b: Lead variants and number of distinct signals in African American-specific association analysis

Locus	Lead Variant	Annotation	P-value	Beta	Effect Allele Frequency	Effect Allele	Number of distinct signals	Sequential Conditioning Lead Variants
LEPR	rs112200619	intronic	1.9E-05	-0.66	0.003	C	0	
IL6R	rs4129267	intronic	1.2E-06	-0.13	0.14	T	1	
CRP	rs112563958	intergenic	8.6E-43	0.32	0.17	T	5	rs4428887, rs3122014, rs11265259, rs181704186
NLRP3	rs56188865	intronic	1.1E-07	-0.09	0.52	C	1	
GCKR	rs556974380	intergenic	8.0E-04	0.50	0.003	C	0	
IL1F10	rs6734238	intergenic	2.2E-06	0.08	0.45	G	1	
HNF1A	rs1169284	intronic	3.6E-06	-0.10	0.24	C	1	
APOE	rs429358	missense, p.Cys130Arg (*APOE4*)	1.3E-21	-0.21	0.21	C	1	

Analysis was performed at 8 loci (500 kb ± genome-wide significant variants) identified in the pooled ancestry analysis. We used the same locus-wide thresholds as pooled ancestry analysis in Table 1.

Table S3: Results from African American and European American stratified analyses for eight signals detected at *CRP* locus in pooled ancestry results (unconditioned).

Signal	Variant	Beta EA	P-value EA	EAF EA	Beta AA	P-value AA	EAF AA	LD with EA leads	LD with AA leads
A	rs7551731	-0.16	2.5E-38	0.33	-0.21	2.5E-23	0.22	r^2=0.93 with rs2211320, lead signal	r^2=0.89 with rs4428887, second signal
B	rs73024795	NA	NA	0.0005	0.33	2.5E-42	0.16		r^2=0.70 with rs112563958, lead signal
C	rs2211321	0.03	5.2E-02	0.71	-0.11	4.9E-09	0.65	r^2=0.98 with rs4425982, fourth signal	r^2=0.36 with rs3122014, third signal
D	rs553202904	-0.71	8.2E-12	0.0031	NA	NA	0.0004	Third signal	
E	rs11265259	NA	NA	0.0004	-0.17	7.3E-08	0.09		Fourth signal
F	rs1800947	-0.24	1.7E-22	0.06	-0.29	4.6E-04	0.01	Second signal	
G	rs12734907	0.10	5.8E-16	0.34	-0.04	0.27	0.08		
H	rs181704186	NA	NA	0.0001	-0.59	3.9E-10	0.01		Fifth signal

We also list the linkage disequilibrium (if r^2>0.2) between the eight *CRP* locus lead variants from the ancestry pooled analysis with the lead *CRP* locus variants identified in ancestry stratified *CRP* locus conditional analyses Five locus-wide significant variants were identified at the *CRP* locus in African Americans, and four locus-wide significant variants were identified at *CRP* in European Americans. Abbreviations: AA, African American; EA, European American; EAF, effect allele frequency; LD, linkage disequilibrium with ancestry stratified conditional analysis results, from European (EUR) (for EA individuals) or African (AFR) (for AA individuals) 1000 Genomes phase 1; NA, not applicable (did not meet 0.1% minor allele frequency threshold). Effect alleles are listed in Table 2.

Table S4: Previous genome-wide significant variants at the C-reactive protein (*CRP*) locus used for conditional analyses

Variant	Position (Chr 1; GRCh38)	Reference	Included in conditional analysis?	r^2<0.9 with other previously identified variants
rs3027012	159,204,333	[5]	Yes	No
rs56288844	159,330,024	[5]	Yes	No
rs6695494	159,603,761	[5]	Yes	No
rs149520992	159,697,727	[5]	Yes	No
rs72698571	159,701,146	[5]	Yes	No
rs12029262	159,709,406	[5]	Yes	No
rs3091244	159,714,875	[5-7]	No (FAIL variant-adjusted for in sensitivity analysis)	-
rs2246469	159,721,022	[5]	Yes	No
rs141729353	159,734,040	[5]	Yes	Yes-kept, removed LD proxies
rs11265263	159,740,727	[5]	Yes	No
rs4131568	159,752,266	[5]	Yes	No
rs3845624	159,248,476	[8]	Yes	No
rs16842484	159,677,134	[6]	Yes	No
rs12093699	159,678,198	[9]	Yes	No
rs10494326	159,679,910	[10]	Yes	No
rs2592887	159,683,149	[6]	Yes	No
rs726640	159,685,728	[11]	Yes	No
rs2592902	159,685,936	[12]	Yes	Yes-removed
rs876537	159,705,143	[13]	Yes	Yes- kept, removed LD proxies
rs16842559	159,706,381	[14]	Yes	Yes-removed
rs2794520	159,709,026	[15]	Yes	Yes- kept, removed LD proxies
rs1800947	159,713,648	[5; 16]	Yes	No
rs77832441	159,714,024	[16]	Yes	No
rs3093059	159,715,346	[17]	Yes	Yes- kept, removed LD proxies
rs1341665	159,721,769	[8]	Yes	Yes- removed
rs2808634	159,722,783	[10]	Yes	Yes-removed
rs7553007	159,728,759	[10]	Yes	Yes- removed
rs11265260	159,730,249	[18]	Yes	Yes- removed

Previously identified variants were identified through review of the literature (particularly [5; 19]). A previously reported tri-allelic variant and the lead *CRP* locus SNP from a multi-ethnic PAGE fine-mapping effort, rs3091244, failed the variant quality filter in TOPMed. We adjusted for the variant calls that were available in a sensitivity analysis, additionally adjusting for all previously identified *CRP* locus variants, and signals E and H from Table 2 remained unchanged (β= -0.32, p= 7.09 x 10^{-18} for rs11265259, β= -0.47, p= 2.89 x 10^{-7} for rs181704186). This variant is also common across ancestry groups and not in high LD with either signal E or H in African ancestry individuals from TOPMed or 1000 Genomes.

We also performed a conditional analysis adjusting only for previously identified *CRP* locus variants with linkage disequilibrium $r^2<0.9$ (as assessed in AA and EA ancestry samples used in TOPMed CRP analysis) with any other previously identified *CRP* variant to prevent potential problems with collinearity. Both signals E and H from Table 2 were still significant in the pooled analysis (β= -0.29, p= 3.57×10^{-16} for rs11265259, β= -0.47, p= 2.55×10^{-7} for rs181704186), and in African Americans alone (β= -0.28, p= 3.13×10^{-13} for rs11265259, β= -0.49, p= 4.64×10^{-6} for rs181704186).

Abbreviations: LD, linkage disequilibrium.

Table S5: Previous genome-wide significant variants at the HNF1 Homeobox A (*HNF1A*) locus used for conditional analyses.

Variant	Position (Chr 12; GRCh38)	Reference	Included in conditional analysis?	r^2<0.9 with other previously identified variants
rs1039302	120,798,455	[20]	Yes	No
rs2650000	120,951,159	[21]	Yes	No
rs7305618	120,965,129	[13]	Yes	No
rs7953249	120,965,921	[22]	Yes	No
rs7979473	120,982,457	[6; 10]	No-FAIL variant	
rs1183910	120,983,004	[23]	Yes	No
rs2393791	120,986,153	[24]	Yes	Yes-kept, removed LD proxies
rs7310409	120,987,058	[5; 17]	Yes	Yes-removed
rs2259816	120,997,784	[10]	Yes	Yes-kept, removed LD proxies
rs1169310	121,001,630	[18]	Yes	Yes-removed
rs2259883	121,024,336	[5]	Yes	No

Previously identified variants were identified through review of the literature (particularly [5; 19]). One previously reported variant was not available for conditional analysis at the *HNF1A* locus (rs7979473[10]), as it failed variant quality filters. However, since both *HNF1A* signals in our analysis were attenuated to non-significance (post-conditioning lead variant rs544759708, $p= 2.69 \times 10^{-5}$, $\beta= -0.46$) even without adjusting for this variant, we did not pursue further conditional analysis adjusting for fail variants. We also did not condition on secondary signal rs2243616 from [6], as it did not meet a conventional genome-wide significance threshold.

We did perform a conditional analysis adjusting only for previously identified *HNF1A* locus variants with linkage disequilibrium $r^2<0.9$ (as assessed in AA and EA ancestry samples used in TOPMed CRP analysis) with any other previously identified *HNF1A* variant to prevent potential problems with collinearity. Results were unchanged (post-conditioning lead variant rs544759708, $p= 2.69 \times 10^{-5}$, $\beta= -0.46$).

Abbreviations: LD, linkage disequilibrium.

Table S6: Linkage disequilibrium between rs11265259 and rs181704186 and previously reported *CRP* locus variants, as well as other signals from TOPMed conditional analysis, in African Americans from the TOPMed CRP analysis

SNP_A	SNP_B	r^2	D'	Source
1:159706154_T/C_rs11265259	1:159724989_T/C_rs7551731	0.028	1	Signal A, our paper
1:159706154_T/C_rs11265259	1:159732996_C/T_rs73024795	0.018	1	Signal B, our paper
1:159706154_T/C_rs11265259	1:159723932_T/C_rs2211321	0.051	1	Signal C, our paper
1:159706154_T/C_rs11265259	1:159738205_A/G_rs553202904	3.63E-05	1	Signal D, our paper
1:159706154_T/C_rs11265259	1:159706154_T/C_rs11265259	1	1	Signal E, our paper
1:159706154_T/C_rs11265259	1:159713648_C/G_rs1800947	0.001	1	Signal F, our paper
1:159706154_T/C_rs11265259	1:159749804_A/T_rs12734907	0.008	1	Signal G, our paper
1:159706154_T/C_rs11265259	1_159204333_T_C	0.004	1	rs3027012
1:159706154_T/C_rs11265259	1_159248476_A_C	0.013	0.97	rs3845624
1:159706154_T/C_rs11265259	1_159330024_A_G	1.75E-04	1	rs56288844
1:159706154_T/C_rs11265259	1_159603761_T_C	0.007	0.31	rs6695494
1:159706154_T/C_rs11265259	1_159677134_C_T	0.114	0.72	rs16842484
1:159706154_T/C_rs11265259	1_159678198_A_G	0.127	0.77	rs12093699
1:159706154_T/C_rs11265259	1_159679910_T_C	0.020	0.97	rs10494326
1:159706154_T/C_rs11265259	1_159683149_T_C	0.086	0.90	rs2592887
1:159706154_T/C_rs11265259	1_159685728_A_G	0.018	0.98	rs726640
1:159706154_T/C_rs11265259	1_159685936_T_G	0.029	0.96	rs2592902
1:159706154_T/C_rs11265259	1_159697727_T_C	1.01E-06	0.09	rs149520992
1:159706154_T/C_rs11265259	1_159701146_T_C	9.21E-04	0.77	rs72698571
1:159706154_T/C_rs11265259	1_159705143_T_C	0.025	1	rs876537
1:159706154_T/C_rs11265259	1_159706381_C_T	0.003	0.97	rs16842559
1:159706154_T/C_rs11265259	1_159709026_T_C	0.026	1	rs2794520
1:159706154_T/C_rs11265259	1_159709406_C_G	0.004	1	rs12029262
1:159706154_T/C_rs11265259	1_159714024_A_G	3.63E-05	1	rs77832441
1:159706154_T/C_rs11265259	1_159715346_G_A	0.271	1	rs3093059
1:159706154_T/C_rs11265259	1_159721022_A_G	0.051	0.98	rs2246469
1:159706154_T/C_rs11265259	1_159721769_A_G	0.026	1	rs1341665
1:159706154_T/C_rs11265259	1_159722783_T_C	0.017	1	rs2808634
1:159706154_T/C_rs11265259	1_159728759_A_G	0.028	1	rs7553007
1:159706154_T/C_rs11265259	1_159730249_G_A	0.007	1	rs11265260
1:159706154_T/C_rs11265259	1_159734040_C_T	0.021	1	rs141729353
1:159706154_T/C_rs11265259	1_159740727_A_C	0.003	1	rs11265263
1:159706154_T/C_rs11265259	1_159752266_T_C	0.008	1	rs4131568

1:159752293_A/G_rs181704186	1:159724989_T/C_rs7551731	0.027	0.96	Signal A, our paper
1:159752293_A/G_rs181704186	1:159732996_C/T_rs73024795	0.001	0.93	Signal B, our paper
1:159752293_A/G_rs181704186	1:159723932_T/C_rs2211321	0.003	0.85	Signal C, our paper
1:159752293_A/G_rs181704186	1:159738205_A/G_rs553202904	0.002	0.19	Signal D, our paper
1:159752293_A/G_rs181704186	1:159706154_T/C_rs11265259	0.001	1	Signal E, our paper
1:159752293_A/G_rs181704186	1:159713648_C/G_rs1800947	8.74E-06	0.003	Signal F, our paper
1:159752293_A/G_rs181704186	1:159749804_A/T_rs12734907	0.001	1	Signal G, our paper
1:159752293_A/G_rs181704186	1_159204333_T_C	3.49E-04	1	rs3027012
1:159752293_A/G_rs181704186	1_159248476_A_C	0.001	1	rs3845624
1:159752293_A/G_rs181704186	1_159330024_A_G	1.31E-04	0.02	rs56288844
1:159752293_A/G_rs181704186	1_159603761_T_C	0.007	0.78	rs6695494
1:159752293_A/G_rs181704186	1_159677134_C_T	0.003	0.93	rs16842484
1:159752293_A/G_rs181704186	1_159678198_A_G	0.003	0.92	rs12093699
1:159752293_A/G_rs181704186	1_159679910_T_C	0.002	1	rs10494326
1:159752293_A/G_rs181704186	1_159683149_T_C	0.009	0.96	rs2592887
1:159752293_A/G_rs181704186	1_159685728_A_G	0.001	0.86	rs726640
1:159752293_A/G_rs181704186	1_159685936_T_G	0.022	0.92	rs2592902
1:159752293_A/G_rs181704186	1_159697727_T_C	2.41E-04	0.04	rs149520992
1:159752293_A/G_rs181704186	1_159701146_T_C	1.78E-05	0.35	rs72698571
1:159752293_A/G_rs181704186	1_159705143_T_C	0.028	0.92	rs876537
1:159752293_A/G_rs181704186	1_159706381_C_T	9.77E-05	0.02	rs16842559
1:159752293_A/G_rs181704186	1_159709026_T_C	0.028	0.93	rs2794520
1:159752293_A/G_rs181704186	1_159709406_C_G	0.198	0.94	rs12029262
1:159752293_A/G_rs181704186	1_159714024_A_G	0.002	0.19	rs77832441
1:159752293_A/G_rs181704186	1_159715346_G_A	0.003	1	rs3093059
1:159752293_A/G_rs181704186	1_159721022_A_G	0.014	0.94	rs2246469
1:159752293_A/G_rs181704186	1_159721769_A_G	0.029	0.96	rs1341665
1:159752293_A/G_rs181704186	1_159722783_T_C	0.002	1	rs2808634
1:159752293_A/G_rs181704186	1_159728759_A_G	0.027	0.96	rs7553007
1:159752293_A/G_rs181704186	1_159730249_G_A	2.57E-05	0.01	rs11265260
1:159752293_A/G_rs181704186	1_159734040_C_T	0.002	1	rs141729353
1:159752293_A/G_rs181704186	1_159740727_A_C	2.37E-04	1	rs11265263
1:159752293_A/G_rs181704186	1_159752266_T_C	7.39E-04	1	rs4131568

Table S7: Women's Health Initiative (WHI) replication analysis

Variant	Beta	P-value	Effect Allele	Effect Allele Frequency	Beta, Post Conditioning	P-value, Post Conditioning	Effect Allele Frequency, 1000G	Beta, 1000G	P-value, 1000G	Beta, Post Conditioning, 1000G	P-value, Post Conditioning, 1000G
rs11265259	-0.18	6.1×10^{-9}	C	0.08	-0.26	8.7×10^{-12}	0.08	-0.17	1.3×10^{-7}	-0.23	2.1×10^{-9}
rs181704186	-0.58	9.2×10^{-11}	G	0.009	-0.45	9.7×10^{-6}	0.008	-0.62	7.1×10^{-11}	-0.50	2.2×10^{-6}

Conditional analysis was done conditioning on all variants in Table S4. Imputation was performed to TOPMed freeze 5b, using the Michigan Imputation Server. Imputation quality was r^2=0.94 and r^2=0.95 for rs181704186 and r^2=0.92 and r^2=0.90 for rs11265259, in two separately analyzed subsets of WHI Affymetrix 6.0 data (one in participants overlapping the Population Architecture using Genomics and Epidemiology (PAGE) MEGA array study (n= 4685) which would have been included in [19], the rest (n=2423) with Affymetrix data only). Imputation quality for all included variants in the conditional analysis was ≥0.6. For the 1000G phase 3 imputation, imputation quality was r^2=0.83 and r^2=0.86 for rs181704186 and r^2=0.77 and r^2=0.81 for rs11265259. Results from the subsets were meta-analyzed with metal (2011-03-25 version).

Table S8a: FUN-LDA tissue specific annotation scores for *CRP* locus variants (signals E and H from Table 2), with top two tissues as well as any additional tissues with an annotation score >0.9 listed.

Epigenome Dataset	Full Name	Score	SNP	Label
E066	Liver	0.0746	rs11265259	CRP, Signal E
E042	Primary T helper 17 cells PMA-I stimulated	0.00006		
E066	Liver	1	rs181704186	CRP, Signal H
E023	Mesenchymal Stem Cell Derived Adipocyte Cultured Cells	0.99977		
E117	HeLa-S3 Cervical Carcinoma Cell Line	0.99907		
E025	Adipose Derived Mesenchymal Stem Cell Cultured Cells	0.98627		
E030	Primary neutrophils from peripheral blood	0.9787		

Table S8b: Annotation PCs for CRP locus variants (signals E and H from Table 2)

rsID	Epigenetics	Conservation	Protein Function	Negative Selection	Distance to Nearest Coding Variant	Mutation Density	Transcription Factor
rs11265259	6.1	18.8	3.0	2.2	1.1	5.0	9.2
rs181704186	10.0	16.3	3.0	3.3	0.3	6.4	18.0

As further described in the methods, we used a novel, multi-dimensional annotation pipeline to derive annotation PCs from individual functional annotations in the following categories: epigenetics, conservation, protein function, negative selection, distance to coding variants, mutation density, and transcription factor binding. Variant-specific annotation PCs are given as the PHRED-scaled scores from the first principal component of the category's individual annotations.

Table S9a: 95% Credible Set Variants for *CRP* locus in European Americans, derived using FINEMAP.

Variants in Credible Set (4 causal variant setting)	
1:159727120_G/C_rs3116653	1:159685936_G/T_rs2592902
1:159728695_C/T_rs3116651	1:159690923_GA/G_rs60702037
1:159731554_C/T_rs3116655	1:159695286_TAA/T_rs3039321
1:159732697_G/A_rs12727021	1:159696131_C/G_rs2808624
1:159743672_A/G_rs74596724	1:159699194_C/T_rs11265257
1:159744970_G/A_rs4656848	1:159705143_C/T_rs876537
1:159748522_A/G_rs4255379	1:159713301_G/A_rs1130864
1:159750926_G/A_rs4420078	1:159713648_C/G_rs1800947
1:159753330_T/C_rs6677719	1:159716693_G/A_rs3116636
1:159753731_G/A_rs4656849	1:159716703_A/G_rs3116635
1:159754730_T/C_rs11265268	1:159719533_T/C_rs3122012
1:159759547_G/C_rs4433388	1:159722054_C/CT_rs35625772
1:159760689_G/T_rs7418263	1:159723815_G/A_rs2211320

Table S9b: 95% Credible Set Variants for *CRP* locus in African Americans, derived using FINEMAP.

Variants in Credible Set (5 causal variant setting)
1:159718685_C/T_rs2808633
1:159723031_G/A_rs2794518
1:159723932_C/T_rs2211321
1:159730897_G/A_rs10797053
1:159741019_G/C_rs10437340
1:159743435_A/T_rs12083620
1:159758337_T/C_rs11265269

Table S10: Oligonucleotide sequences for functional assays. Forward and reverse oligonucleotides indicate forward or reverse directions (5'-3') with respect to the genome.

PCR primers for reporter assays	**Sequence (5'-3')**	**Region (hg19)**
rs181704186 Forward	TTCATGGGGCAGATGATACA	chr1:159,721,514-159,722,654
rs181704186 Reverse	GGCATGTTGTCTTGCAGGTA	
Oligonucleotide sequences for EMSAs		
rs181704186 Forward	AGTTGCACA/GATGGGAGG	chr1:159,722,075-159,722,091
rs181704186 Reverse	CCTCCCATT/CGTGCAACT	

Supplemental Materials and Methods

Statistical Analysis

Our analysis included 23,279 individuals [average age 59.2 years; 32% male; predominantly European (64.7%) and African American (28.1%) ancestry] from nine cohorts. Inverse-normalized natural log-transformed CRP values were assessed. Models were adjusted for sex, age, study, and self-reported ancestry, as well as ten cross-cohort ancestry principal components calculated from 228,497 LD pruned variants (r^2<0.1 across all freeze 5b individuals) with a minor allele frequency >1%. For each cohort, basic demographic, self-reported ancestry sub-group, and assay information is displayed in Table S1. Individuals with raw CRP levels of zero or residual values more than 3 standard deviations outside the mean were excluded.

We analyzed variants and indels with a minor allele frequency >0.1% (corresponding to a minor allele count >46 in our pooled ancestry sample) using WGS data from freeze 5b (see https://www.nhlbiwgs.org/topmed-whole-genome-sequencing-project-freeze-5b-phases-1-and-2 and preprint at[25] for sequencing and variant calling methods). We used EPACTS (v3.3.3) on the University of Michigan ENCORE server for initial analyses with EMMAX to control for sample relatedness. Stepwise conditional analysis at each identified locus was performed locally using the same EPACTS version. Loci were declared significant at a threshold of $p<1x10^{-9}$ based on estimated number of independent tests for whole genome sequencing data[26]. Within an identified locus (500 kb on each side of any variant with $p<1 \times 10^{-9}$), we defined a Bonferroni corrected p-value threshold based on the number of tested variants. This threshold is conservative given the correlation between variants within a locus, but increases our confidence in the robustness of identified distinct signals. We then performed stepwise conditional analysis to define the number of conditionally distinct signals at each locus, defined as the number of rounds of conditional analysis needed to have no variants within the locus with a p-values lower than the locus threshold. We also performed analyses adjusting for variants previously attaining genome-wide significance at the *CRP* (Table S4) and *HNF1A* loci (Table S5). Conditional analyses at the *CRP* locus were visualized using LocusZoom, using linkage disequilibrium calculated from included TOPMed subjects[27].

We performed statistical fine-mapping with FINEMAP (v1.3.1)[28] using marginal test statistics and TOPMed derived LD reference panels in unrelated EA and AA participants from TOPMed (selected from individuals included in TOPMed CRP analysis using PC-air, n=4,442 AAs, n=11,397 EAs). We chose FINEMAP specifically because it permits a large number of potential causal variants at a locus. At the CRP locus, we input a maximum of 5 causal variants in our sample of AAs and 4 causal variants in EAs, based on the number of conditionally distinct signals from stepwise conditional analysis.

Annotation

For signals E and H, we used the FUN-LDA program (functional effect prediction for noncoding variants, using a latent Dirichlet allocation model) to identify the tissue type in which they were most likely to have a functional effect[29]. This program gives each variant a score ranging from 0 to 1 (with higher scores indicating variants that are most likely to be functional) based on epigenetic assays evidence, with scores available for 127 cell types and tissues in Roadmap Epigenomics. FUN-LDA scores are derived by summing posterior probabilities for active functional classes (such as promoters and enhancers), based on histone modifications and quantitative DNAse hypersensitivity.

We also used a novel, multi-dimensional annotation pipeline, which derives annotation PCs from individual functional annotations in the following categories: epigenetics, conservation, protein function, negative selection, distance to coding variants, mutation

density, and transcription factor binding. Variant-specific annotation PCs are given as the PHRED-scaled scores from the first principal component of the category's individual annotations. Values greater than 10 thus represent variants in the top 10% of a given annotation category. We report the epigenetic PC calculated from individual annotations percent GC within +/- 75bp window, percent CpG within +/- 75bp window, maximum Encode H3K4me1 level, maximum Encode H3K4me2 level, maximum Encode H3K4me3 level, maximum Encode H3K9ac level, maximum Encode H3K9me3 level, maximum Encode H3K27ac level, maximum Encode H3K27me3 level, maximum Encode H3K36me3, maximum Encode H3K79me2 level, maximum Encode H4K20me1 level, maximum Encode EncodeH2AFZ level, ReMap count of binding transcription factors, ReMap count of binding transcription factors for cell line combinations, distance to nearest Transcribed Sequence Start (TSS), and distance to nearest Transcribed Sequence End (TSE). We also report conservation PC calculated from the neutral evolution score of GERP++, rejected Substitution score of GERP++, primate PhastCons conservation score, mammalian PhastCons conservation score, vertebrate PhastCons conservation score, primate PhyloP score, mammalian PhyloP score, and the vertebrate PhyloP score. All annotations are drawn from CADD database[30]. Finally, we assessed whether lead CRP-associated variants were colocalized (r^2>0.8 in EUR or AFR populations; 1000 Genomes phase 3) with lead variants from eQTL signals from GTEx (all tissues[31]) or eQTLGen (whole blood)[32] (https://www.eqtlgen.org/index.html) or a recent large adult liver eQTL analysis[33]. We also examined GeneHancer for enhancer/gene pairings, as determined based on scores for tissue co-expression correlation between genes and enhancer RNAs, enhancer-targeted transcription factor genes, eQTLs for variants within enhancers, and promoter capture Hi-C[34].

Replication

African American individuals with Affymetrix 6.0 data from the WHI[35] SHARe resource (dbGaP phs000386.v7.p3) were imputed using TOPMed freeze 5b as a reference panel. We then performed association analysis for inverse-normalized natural log-transformed CRP in the *CRP* region using the EMMAX test in EPACTS v3.2.6, adjusting for an empirical kinship matrix and age. We also performed an additional analysis adjusting for known *CRP* locus variants from GWAS and exome sequencing analyses.

PheWAS

We additionally performed a follow-up phenome-wide association study (pheWAS) for rs181704186 and rs11265259 in BioVU. BioVU is the biobank of Vanderbilt University Medical Center (VUMC) that houses de-identified DNA samples linked to phenotypic data derived from electronic health records (EHRs) system of VUMC. DNA samples were genotyped with genome-wide arrays including the Multi-Ethnic Global **(**MEGA) array, and the genotype data were imputed into the HRC reference panel using the Michigan imputation server. In total, 1815 phecodes (i.e., groupings of ICD codes into clinically similar diseases or traits) were tested for association in up to 5275 African Americans. Association between each binary phecode and a SNP was assessed using logistic regression, while adjusting for covariates of age, gender, genotyping array type/batch and 10 principal components of ancestry.

Functional Assays

Cell Culture HepG2 human liver carcinoma cells were cultured in MEM-alpha (Corning) supplemented with 10% FBS, 2 mM L-glutamine, and 1 mM sodium pyruvate. Cells were maintained at 37°C in 5% CO_2.

Transcriptional Reporter Assays Oligonucleotide primers (Table S10) containing KpnI and XhoI restriction sites were designed to PCR-amplify a 1,141-bp region (GRCh37/hg19 –chr1:159,721,514 – 159,722,654) surrounding rs181704186. A DNA segment from an individual homozygous for rs181704186-A was amplified, digested with KpnI and XhoI, and ligated into the minimal promoter-containing luciferase reporter vector pGL4.23 (Promega). The constructs were altered to create vectors containing the low-frequency rs181704186-G allele using the QuikChange site-directed mutagenesis kit (Stratagene). Isolated clones were sequenced for genotype and fidelity.

1.3×10^5 HepG2 cells per well were seeded in 24-well plates. Cells were co-transfected using Lipofectamine 3000 (Life Technologies) with five independent pGL4.23 constructs and *Renilla* luciferase vector phRL-TK (Promega) to control for transfection efficiency. 48 hours post-transfection, cells were lysed with Passive Lysis Buffer (Promega) and measured for luciferase activity using the Dual-Luciferase Reporter Assay system (Promega) as directed and previously described[36]. Reporter assays were repeated on a second separate day and yielded comparable results.

Electrophoretic Mobility Shift Assays Nuclear protein was extracted from HepG2 cells using the NE-PER Nuclear and Cytoplasmic Extraction Kit (Thermo Scientific). Biotinylated and unlabeled 17-bp oligonucleotide probes (Table S10) were designed centered around rs181704186 and annealed as previously described[36]. Electrophoretic Mobility Shift Assays (EMSAs) were performed using the LightShift Chemiluminescent EMSA Kit (Thermo Fisher Scientific). 20 uL binding reactions containing 10 ug nuclear protein, 400 fmol labeled probe, 1x binding buffer, and 50 ng/uL poly(dI-dC) were incubated at room temperature for 25 minutes. For competition reactions, 40-fold excess of unlabeled probe was incubated in the reaction for 15 minutes prior to addition of the labeled probe, followed by 25 minutes of incubation. Gel electrophoresis and transfer, wash, and detection steps were performed as previously described[37]. EMSAs were carried out on a second separate day and yielded comparable results.

Supplemental Acknowledgements
Whole genome sequencing (WGS) for the Trans-Omics in Precision Medicine (TOPMed) program was supported by the National Heart, Lung and Blood Institute (NHLBI). WGS for "NHLBI TOPMed: Whole Genome Sequencing and Related Phenotypes in the Framingham Heart Study" (phs000974) was performed at the Broad Institute of MIT and Harvard (3U54HG003067-12S2). WGS for "NHLBI TOPMed: The Jackson Heart Study" (phs000964) was performed at the University of Washington Northwest Genomics Center (HHSN268201100037C). WGS for "NHLBI TOPMed: Genetic Epidemiology of COPD (COPDGene) in the TOPMed Program" (phs000951) was performed at the Broad Institute (HHSN268201500014C) and the University of Washington Northwest Genomics Center [3R01HL089856-08S, Phase 2 at The Broad Institute]. WGS for "NHLBI TOPMed: Genetics of Cardiometabolic Health in the Amish" (phs000956) was performed at the Broad Institute (3R01HL121007-01S1). WGS for "NHLBI TOPMed: Trans-Omics for Precision Medicine Whole Genome Sequencing Project: ARIC" (phs001211) was performed at Baylor and the Broad Institute [3R01HL092577-06S1 (The Broad Institute, AFGen), HHSN268201500015C (Baylor, VTE), 3U54HG003273-12S2 (Baylor, VTE)]. WGS for "NHLBI TOPMed: GeneSTAR (Genetic Study of Atherosclerosis Risk)" (phs001218) was performed at Macrogen (3R01HL112064-04S1), Illumina (R01HL112064), and the Broad Institute [HHSN268201500014C (The Broad Institute, AA_CAC)].

WGS for “NHLBI TOPMed: MESA and MESA Family AA-CAC” (phs001416) was performed at the Broad Institute [3U54HG003067-13S1 (MESA, TOPMed supplement to NHGRI), HHSN268201500014C (The Broad Institute, AA_CAC)]. WGS for “NHLBI TOPMed: Women's Health Initiative (WHI)” (phs001237) was performed at the Broad Institute (HHSN268201500014C). WGS for “NHLBI TOPMed: The Cleveland Family Study (WGS)” (phs000954) was performed at the University of Washington Northwest Genomics Center (3R01HL098433-05S1). Centralized read mapping and genotype calling along with variant quality metrics and filtering were provided by the TOPMed Informatics Research Center (3R01HL-117626-02S1; contract HHSN268201800002I). Phenotype harmonization, data management, sample-identity QC, and general study coordination, were provided by the TOPMed Data Coordinating Center (3R01HL-120393-02S1; contract HHSN268201800001I). We gratefully acknowledge the studies and participants who provided biological samples and data for TOPMed.

The WHI program is funded by the National Heart, Lung, and Blood Institute, National Institutes of Health, U.S. Department of Health and Human Services through contracts HHSN268201100046C, HHSN268201100001C, HHSN268201100002C, HHSN268201100003C, HHSN268201100004C, and HHSN271201100004C. The authors thank the WHI investigators and staff for their dedication, and the study participants for making the program possible. A listing of WHI investigators can be found at: https://www.whi.org/researchers/Documents%20%20Write%20a%20Paper/WHI%20Investigator%20Long%20List.pdf.

The Jackson Heart Study (JHS) is supported and conducted in collaboration with Jackson State University (HHSN268201800013I), Tougaloo College (HHSN268201800014I), the Mississippi State Department of Health (HHSN268201800015I/HHSN26800001) and the University of Mississippi Medical Center (HHSN268201800010I, HHSN268201800011I and HHSN268201800012I) contracts from the National Heart, Lung, and Blood Institute (NHLBI) and the National Institute for Minority Health and Health Disparities (NIMHD). The authors also wish to thank the staffs and participants of the JHS.

MESA and the MESA SHARe project are conducted and supported by the National Heart, Lung, and Blood Institute (NHLBI) in collaboration with MESA investigators. Support for MESA is provided by contracts HHSN268201500003I, N01-HC-95159, N01-HC-95160, N01-HC-95161, N01-HC-95162, N01-HC-95163, N01-HC-95164, N01-HC-95165, N01-HC-95166, N01-HC-95167, N01-HC-95168, N01-HC-95169, UL1-TR-000040, UL1-TR-001079, UL1-TR-001420, UL1-TR-001881, and DK063491. MESA Family is conducted and supported by the National Heart, Lung, and Blood Institute (NHLBI) in collaboration with MESA investigators. Support is provided by grants and contracts R01HL071051, R01HL071205, R01HL071250, R01HL071251, R01HL071258, R01HL071259, and by the National Center for Research Resources, Grant UL1RR033176. The provision of genotyping data was supported in part by the National Center for Advancing Translational Sciences, CTSI grant UL1TR001881, and the National Institute of Diabetes and Digestive and Kidney Disease Diabetes Research Center (DRC) grant DK063491 to the Southern California Diabetes Endocrinology Research Center.

The COPDGene project described was supported by Award Number U01 HL089897, U01 HL089856, R01 HL095432, and R01 HL129937 from the National Heart, Lung, and Blood Institute. The content is solely the responsibility of the authors and does not necessarily represent the official views of the National Heart, Lung, and Blood Institute or the National Institutes of Health. The

COPDGene project is also supported by the COPD Foundation through contributions made to an Industry Advisory Board comprised of AstraZeneca, Boehringer Ingelheim, GlaxoSmithKline, Novartis, Pfizer, Siemens and Sunovion. A full listing of COPDGene investigators can be found at: http://www.copdgene.org/directory

GeneSTAR was supported by the National Institutes of Health/National Heart, Lung, and Blood Institute (U01 HL72518, HL087698, HL112064, HL11006, HL118356) and by a grant from the National Institutes of Health/National Center for Research Resources (M01-RR000052) to the Johns Hopkins General Clinical Research Center.

The Framingham Heart Study inflammation work was supported by HHSN268201500001I, N01-HC 25195, 75N92019D00031, 1RO1 HL64753, R01 HL076784, and 1 R01 AG028321.

The Cleveland Family Study has been supported by National Institutes of Health grants [R01-HL046380, KL2-RR024990, R35-HL135818, HL 046389, HL113338, R35HL135818 and R01-HL113338].

The TOPMed component of the Amish Research Program was supported by NIH grants R01 HL121007, U01 HL072515, and R01 AG18728.

The Atherosclerosis Risk in Communities study has been funded in whole or in part with Federal funds from the National Heart, Lung, and Blood Institute, National Institutes of Health, Department of Health and Human Services (contract numbers HHSN268201700001I, HHSN268201700002I, HHSN268201700003I, HHSN268201700004I and HHSN268201700005I). The authors thank the staff and participants of the ARIC study for their important contributions.

The views expressed in this manuscript are those of the authors and do not necessarily represent the views of the National Heart, Lung, and Blood Institute; the National Institutes of Health; or the U.S. Department of Health and Human Services.

Support for title page creation and format was provided by AuthorArranger, a tool developed at the National Cancer Institute.

We used the OASIS (Omics Analysis, Search and Information System) tool for initial exploration of our TOPMed association results for C-reactive protein. OASIS is a web-based platform for mining and visualizing omics association analysis results (and thus enabling the transformation of massive volumes of “results data” into a more complete understanding of biology). OASIS resources, video library and contact information available from https://edn.som.umaryland.edu/OASIS/.

Supplementary References

1. Whelton, S.P., Roy, P., Astor, B.C., Zhang, L., Hoogeveen, R.C., Ballantyne, C.M., and Coresh, J. (2013). Elevated high-sensitivity C-reactive protein as a risk marker of the attenuated relationship between serum cholesterol and cardiovascular events at older age. The ARIC Study. American Journal of Epidemiology 178, 1076-1084.

2. Sun, W., Kechris, K., Jacobson, S., Drummond, M.B., Hawkins, G.A., Yang, J., Chen, T.-h., Quibrera, P.M., Anderson, W., Barr, R.G., et al. (2016). Common Genetic Polymorphisms Influence Blood Biomarker Measurements in COPD. PLoS genetics 12, e1006011.
3. Fox, E.R., Benjamin, E.J., Sarpong, D.F., Rotimi, C.N., Wilson, J.G., Steffes, M.W., Chen, G., Adeyemo, A., Taylor, J.K., Samdarshi, T.E., et al. (2008). Epidemiology, heritability, and genetic linkage of C-reactive protein in African Americans (from the Jackson Heart Study). Am J Cardiol 102, 835-841.
4. Mann, D.M., Shimbo, D., Cushman, M., Lakoski, S., Greenland, P., Blumenthal, R.S., Michos, E.D., Lloyd-Jones, D.M., and Muntner, P. (2013). C-reactive protein level and the incidence of eligibility for statin therapy: the multi-ethnic study of atherosclerosis. Clinical cardiology 36, 15-20.
5. Ligthart, S., Vaez, A., Võsa, U., Stathopoulou, M.G., de Vries, P.S., Prins, B.P., Van der Most, P.J., Tanaka, T., Naderi, E., Rose, L.M., et al. (2018). Genome Analyses of >200,000 Individuals Identify 58 Loci for Chronic Inflammation and Highlight Pathways that Link Inflammation and Complex Disorders. The American Journal of Human Genetics 103, 691-706.
6. Kocarnik, J.M., Richard, M., Graff, M., Haessler, J., Bien, S., Carlson, C., Carty, C.L., Reiner, A.P., Avery, C.L., Ballantyne, C.M., et al. (2018). Discovery, fine-mapping, and conditional analyses of genetic variants associated with C-reactive protein in multiethnic populations using the Metabochip in the Population Architecture using Genomics and Epidemiology (PAGE) study. Human molecular genetics 27, 2940-2953.
7. Ridker, P., Pare, G., Parker, A., Zee, R., Danik, J., Buring, J., Kwiatkowski, D., Cook, N., Miletich, J., and Chasman, D. (2008). Loci related to metabolic-syndrome pathways including LEPR,HNF1A, IL6R, and GCKR associate with plasma C-reactive protein: the Women's Genome Health Study. American journal of human genetics 82, 1185-1192.
8. Naitza, S., Porcu, E., Steri, M., Taub, D.D., Mulas, A., Xiao, X., Strait, J., Dei, M., Lai, S., Busonero, F., et al. (2012). A genome-wide association scan on the levels of markers of inflammation in Sardinians reveals associations that underpin its complex regulation. PLoS genetics 8, e1002480.
9. Melzer, D., Perry, J.R., Hernandez, D., Corsi, A.M., Stevens, K., Rafferty, I., Lauretani, F., Murray, A., Gibbs, J.R., Paolisso, G., et al. (2008). A genome-wide association study identifies protein quantitative trait loci (pQTLs). PLoS genetics 4, e1000072.
10. Reiner A , P., Beleza, S., Franceschini, N., Auer P , L., Robinson J , G., Kooperberg, C., Peters, U., and Tang, H. (2012). Genome-wide Association and Population Genetic Analysis of C-Reactive Protein in African American and Hispanic American Women. Am J Hum Genet 91, 502-512.
11. Doumatey, A.P., Chen, G., Tekola Ayele, F., Zhou, J., Erdos, M., Shriner, D., Huang, H., Adeleye, J., Balogun, W., Fasanmade, O., et al. (2012). C-reactive protein (CRP) promoter polymorphisms influence circulating CRP levels in a genome-wide association study of African Americans. Hum Mol Genet 21, 3063-3072.
12. Williams, S.R., Hsu, F.C., Keene, K.L., Chen, W.M., Nelson, S., Southerland, A.M., Madden, E.B., Coull, B., Gogarten, S.M., Furie, K.L., et al. (2016). Shared genetic susceptibility of vascular-related biomarkers with ischemic and recurrent stroke. Neurology 86, 351-359.
13. Wu, Y., McDade, T.W., Kuzawa, C.W., Borja, J., Li, Y., Adair, L.S., Mohlke, K.L., and Lange, L.A. (2012). Genome-wide association with C-reactive protein levels in CLHNS: evidence for the CRP and HNF1A loci and their interaction with exposure to a pathogenic environment. Inflammation 35, 574-583.

14. Dorajoo, R., Li, R., Ikram, M.K., Liu, J., Froguel, P., Lee, J., Sim, X., Ong, R.T., Tay, W.T., Peng, C., et al. (2013). Are C-reactive protein associated genetic variants associated with serum levels and retinal markers of microvascular pathology in Asian populations from Singapore? PloS one 8, e67650.
15. Dehghan, A., Dupuis, J., Barbalic, M., Bis, J.C., Eiriksdottir, G., Lu, C., Pellikka, N., Wallaschofski, H., Kettunen, J., Henneman, P., et al. (2011). Meta-analysis of genome-wide association studies in >80 000 subjects identifies multiple loci for C-reactive protein levels. Circulation 123, 731-738.
16. Schick, U.M., Auer, P.L., Bis, J.C., Lin, H., Wei, P., Pankratz, N., Lange, L.A., Brody, J., Stitziel, N.O., Kim, D.S., et al. (2015). Association of exome sequences with plasma C-reactive protein levels in >9000 participants. Hum Mol Genet 24, 559-571.
17. Okada, Y., Takahashi, A., Ohmiya, H., Kumasaka, N., Kamatani, Y., Hosono, N., Tsunoda, T., Matsuda, K., Tanaka, T., Kubo, M., et al. (2011). Genome-wide association study for C-reactive protein levels identified pleiotropic associations in the IL6 locus. Hum Mol Genet 20, 1224-1231.
18. Reiner, A.P., Barber, M.J., Guan, Y., Ridker, P.M., Lange, L.A., Chasman, D.I., Walston, J.D., Cooper, G.M., Jenny, N.S., Rieder, M.J., et al. (2008). Polymorphisms of the HNF1A gene encoding hepatocyte nuclear factor-1 alpha are associated with C-reactive protein. Am J Hum Genet 82, 1193-1201.
19. Wojcik, G.L., Graff, M., Nishimura, K.K., Tao, R., Haessler, J., Gignoux, C.R., Highland, H.M., Patel, Y.M., Sorokin, E.P., Avery, C.L., et al. (2019). Genetic analyses of diverse populations improves discovery for complex traits. Nature 570, 514-518.
20. Lowe, J.K., Maller, J.B., Pe'er, I., Neale, B.M., Salit, J., Kenny, E.E., Shea, J.L., Burkhardt, R., Smith, J.G., Ji, W., et al. (2009). Genome-wide association studies in an isolated founder population from the Pacific Island of Kosrae. PLoS genetics 5, e1000365.
21. Kocarnik, J.M., Pendergrass, S.A., Carty, C.L., Pankow, J.S., Schumacher, F.R., Cheng, I., Durda, P., Ambite, J.L., Deelman, E., Cook, N.R., et al. (2014). Multiancestral analysis of inflammation-related genetic variants and C-reactive protein in the population architecture using genomics and epidemiology study. Circulation Cardiovascular genetics 7, 178-188.
22. Kim, D.K., Cho, M.H., Hersh, C.P., Lomas, D.A., Miller, B.E., Kong, X., Bakke, P., Gulsvik, A., Agusti, A., Wouters, E., et al. (2012). Genome-wide association analysis of blood biomarkers in chronic obstructive pulmonary disease. American journal of respiratory and critical care medicine 186, 1238-1247.
23. Elliott, P., Chambers, J.C., Zhang, W., Clarke, R., Hopewell, J.C., Peden, J.F., Erdmann, J., Braund, P., Engert, J.C., Bennett, D., et al. (2009). Genetic Loci associated with C-reactive protein levels and risk of coronary heart disease. Jama 302, 37-48.
24. Vinayagamoorthy, N., Hu, H.J., Yim, S.H., Jung, S.H., Jo, J., Jee, S.H., and Chung, Y.J. (2014). New variants including ARG1 polymorphisms associated with C-reactive protein levels identified by genome-wide association and pathway analysis. PloS one 9, e95866.
25. Taliun, D., Harris, D.N., Kessler, M.D., Carlson, J., Szpiech, Z.A., Torres, R., Taliun, S.A.G., Corvelo, A., Gogarten, S.M., Kang, H.M., et al. (2019). Sequencing of 53,831 diverse genomes from the NHLBI TOPMed Program. bioRxiv, 563866.
26. Pulit, S.L., de With, S.A., and de Bakker, P.I. (2017). Resetting the bar: Statistical significance in whole-genome sequencing-based association studies of global populations. Genetic epidemiology 41, 145-151.
27. Pruim, R.J., Welch, R.P., Sanna, S., Teslovich, T.M., Chines, P.S., Gliedt, T.P., Boehnke, M., Abecasis, G.R., and Willer, C.J. (2010). LocusZoom: regional visualization of genome-wide association scan results. Bioinformatics 26, 2336-2337.

28. Benner, C., Spencer, C.C., Havulinna, A.S., Salomaa, V., Ripatti, S., and Pirinen, M. (2016). FINEMAP: efficient variable selection using summary data from genome-wide association studies. Bioinformatics 32, 1493-1501.
29. Backenroth, D., He, Z., Kiryluk, K., Boeva, V., Pethukova, L., Khurana, E., Christiano, A., Buxbaum, J.D., and Ionita-Laza, I. (2018). FUN-LDA: A Latent Dirichlet Allocation Model for Predicting Tissue-Specific Functional Effects of Noncoding Variation: Methods and Applications. American journal of human genetics 102, 920-942.
30. Rentzsch, P., Witten, D., Cooper, G.M., Shendure, J., and Kircher, M. (2019). CADD: predicting the deleteriousness of variants throughout the human genome. Nucleic acids research 47, D886-d894.
31. Gamazon, E.R., Segre, A.V., van de Bunt, M., Wen, X., Xi, H.S., Hormozdiari, F., Ongen, H., Konkashbaev, A., Derks, E.M., Aguet, F., et al. (2018). Using an atlas of gene regulation across 44 human tissues to inform complex disease- and trait-associated variation. Nat Genet 50, 956-967.
32. Võsa, U., Claringbould, A., Westra, H.-J., Bonder, M.J., Deelen, P., Zeng, B., Kirsten, H., Saha, A., Kreuzhuber, R., Kasela, S., et al. (2018). Unraveling the polygenic architecture of complex traits using blood eQTL metaanalysis. bioRxiv, 447367.
33. Strunz, T., Grassmann, F., Gayan, J., Nahkuri, S., Souza-Costa, D., Maugeais, C., Fauser, S., Nogoceke, E., and Weber, B.H.F. (2018). A mega-analysis of expression quantitative trait loci (eQTL) provides insight into the regulatory architecture of gene expression variation in liver. Scientific reports 8, 5865.
34. Fishilevich, S., Nudel, R., Rappaport, N., Hadar, R., Plaschkes, I., Iny Stein, T., Rosen, N., Kohn, A., Twik, M., Safran, M., et al. (2017). GeneHancer: genome-wide integration of enhancers and target genes in GeneCards. Database : the journal of biological databases and curation 2017.
35. The Women's Health Initiative Study Group. (1998). Design of the Women's Health Initiative clinical trial and observational study. Control Clin Trials 19, 61-109.
36. Fogarty, M.P., Cannon, M.E., Vadlamudi, S., Gaulton, K.J., and Mohlke, K.L. (2014). Identification of a Regulatory Variant That Binds FOXA1 and FOXA2 at the CDC123/CAMK1D Type 2 Diabetes GWAS Locus. PLoS genetics 10, e1004633.
37. Roman, T.S., Cannon, M.E., Vadlamudi, S., Buchkovich, M.L., Wolford, B.N., Welch, R.P., Morken, M.A., Kwon, G.J., Varshney, A., Kursawe, R., et al. (2017). A Type 2 Diabetes-Associated Functional Regulatory Variant in a Pancreatic Islet Enhancer at the ADCY5 Locus. Diabetes 66, 2521-2530.

TOPMed Banner Authors

Name	Institution(s)	Primary Department	Institution City	Institution State	Zip Code	Country
Abe, Namiko	New York Genome Center		New York	New York	10013	US
Abecasis, Gonçalo	University of Michigan		Ann Arbor	Michigan	48109	US
Albert, Christine	Massachusetts General Hospital		Boston	Massachusetts	02114	US

Almasy, Laura	Children's Hospital of Philadelphia, University of Pennsylvania		Philadelphia	Pennsylvania	19104	US
Alonso, Alvaro	Emory University		Atlanta	Georgia	30322	US
Ament, Seth	University of Maryland		Baltimore	Maryland	21201	US
Anderson, Peter	University of Washington		Seattle	Washington	98195	US
Anugu, Pramod	University of Mississippi		Jackson	Mississippi	38677	US
Applebaum-Bowden, Deborah	National Institutes of Health		Bethesda	Maryland	20892	US
Arking, Dan	Johns Hopkins University		Baltimore	Maryland	21218	US
Arnett, Donna K	University of Kentucky		Lexington	Kentucky	40506	US
Ashley-Koch, Allison	Duke University		Durham	North Carolina	27708	US
Aslibekyan, Stella	University of Alabama		Birmingham	Alabama	35487	US
Assimes, Tim	Stanford University		Stanford	California	94305	US
Auer, Paul	University of Wisconsin Milwaukee		Milwaukee	Wisconsin	53211	US
Avramopoulos, Dimitrios	Johns Hopkins University		Baltimore	Maryland	21218	US
Barnard, John	Cleveland Clinic		Cleveland	Ohio	44195	US
Barnes, Kathleen	University of Colorado at Denver		Denver	Colorado	80204	US
Barr, R. Graham	Columbia University		New York	New York	10027	US
Barron-Casella, Emily	Johns Hopkins University		Baltimore	Maryland	21218	US
Beaty, Terri	Johns Hopkins University		Baltimore	Maryland	21218	US
Becker, Diane	Johns Hopkins University		Baltimore	Maryland	21218	US
Becker, Lewis	Johns Hopkins University		Baltimore	Maryland	21218	US

Beer, Rebecca	National Heart, Lung, and Blood Institute, National Institutes of Health		Bethesda	Maryland	20892	US
Begum, Ferdouse	Johns Hopkins University		Baltimore	Maryland	21218	US
Beitelshees, Amber	University of Maryland		Baltimore	Maryland	21201	US
Benjamin, Emelia	Boston University, Massachusetts General Hospital	Boston University School of Medicine	Boston	Massachusetts	02118	US
Bezerra, Marcos	Fundação de Hematologia e Hemoterapia de Pernambuco - Hemope		Recife		52011-000	BR
Bielak, Larry	University of Michigan		Ann Arbor	Michigan	48109	US
Bis, Joshua	University of Washington		Seattle	Washington	98195	US
Blackwell, Thomas	University of Michigan		Ann Arbor	Michigan	48109	US
Blangero, John	University of Texas Rio Grande Valley School of Medicine	Human Genetics	Brownsville	Texas	78520	US
Boerwinkle, Eric	University of Texas Health at Houston		Houston	Texas	77225	US
Bowden, Donald W.	Wake Forest Baptist Health	Department of Biochemistry	Winston-Salem	North Carolina	27157	US
Bowler, Russell	National Jewish Health	National Jewish Health	Denver	Colorado	80206	US
Brody, Jennifer	University of Washington		Seattle	Washington	98195	US
Broeckel, Ulrich	Medical College of Wisconsin		Milwaukee	Wisconsin	53226	US
Broome, Jai	University of Washington		Seattle	Washington	98195	US

Bunting, Karen	New York Genome Center		New York	New York	10013	US
Burchard, Esteban	University of California, San Francisco		San Francisco	California	94143	US
Buth, Erin	University of Washington	Biostatistics	Seattle	Washington	98195	US
Cade, Brian	Brigham & Women's Hospital	Brigham and Women's Hospital	Boston	Massachusetts	02115	US
Cardwell, Jonathan	University of Colorado at Denver		Denver	Colorado	80204	US
Carty, Cara	Women's Health Initiative		Seattle	Washington	98109	US
Casaburi, Richard	University of California, Los Angeles		Los Angeles	California	90095	US
Casella, James	Johns Hopkins University		Baltimore	Maryland	21218	US
Chaffin, Mark	Broad Institute		Cambridge	Massachusetts	02142	US
Chang, Christy	University of Maryland		Baltimore	Maryland	21201	US
Chasman, Daniel	Brigham & Women's Hospital		Boston	Massachusetts	02115	US
Chavan, Sameer	University of Colorado at Denver		Denver	Colorado	80204	US
Chen, Bo-Juen	New York Genome Center		New York	New York	10013	US
Chen, Wei-Min	University of Virginia		Charlottesville	Virginia	22903	US
Chen, Yii-Der Ida	Los Angeles Biomedical Research Institute		Charlottesville	Virginia	90502	US
Cho, Michael	Brigham & Women's Hospital		Boston	Massachusetts	02115	US
Choi, Seung Hoan	Broad Institute		Cambridge	Massachusetts	02142	US
Chuang, Lee-Ming	National Taiwan University	National Taiwan University Hospital	Taipei		10617	TW

Chung, Mina	Cleveland Clinic		Cleveland	Ohio	44195	US
Conomos, Matthew	University of Washington	Biostatistics	Seattle	Washington	98115	US
Cornell, Elaine	University of Vermont		Burlington	Vermont	05405	US
Correa, Adolfo	University of Mississippi	Medicine	Jackson	Mississippi	39216	US
Crandall, Carolyn	University of California, Los Angeles		Los Angeles	California	90095	US
Crapo, James	National Jewish Health		Denver	Colorado	80206	US
Cupples, L. Adrienne	Boston University		Boston	Massachusetts	02215	US
Curran, Joanne	University of Texas Rio Grande Valley School of Medicine		Brownsville	Texas	78520	US
Curtis, Jeffrey	University of Michigan		Ann Arbor	Michigan	48109	US
Custer, Brian	Vitalant Research Institute		San Francisco	California	94118	US
Damcott, Coleen	University of Maryland		Baltimore	Maryland	21201	US
Darbar, Dawood	University of Illinois at Chicago		Chicago	Illinois	60607	US
Das, Sayantan	University of Michigan		Ann Arbor	Michigan	48109	US
David, Sean	Stanford University		Stanford	California	94305	US
Davis, Colleen	University of Washington		Seattle	Washington	98195	US
Daya, Michelle	University of Colorado at Denver		Denver	Colorado	80204	US
de Andrade, Mariza	Mayo Clinic		Rochester	Minnesota	55905	US
DeBaun, Michael	Vanderbilt University		Nashville	Tennessee	37235	US
Deka, Ranjan	University of Cincinnati		Cincinnati	Ohio	45220	US
DeMeo, Dawn	Brigham & Women's Hospital		Boston	Massachusetts	02115	US
Devine, Scott	University of Maryland		Baltimore	Maryland	21201	US

Do, Ron	Icahn School of Medicine at Mount Sinai		New York	New York	10029	US
Duan, Qing	University of North Carolina		Chapel Hill	North Carolina	27599	US
Duggirala, Ravi	University of Texas Rio Grande Valley School of Medicine		Edinburg	Texas	78539	US
Durda, Jon Peter	University of Vermont		Burlington	Vermont	05405	US
Dutcher, Susan	Washington University in St Louis		St Louis	Missouri	63130	US
Eaton, Charles	Brown University		Providence	Rhode Island	02912	US
Ekunwe, Lynette	University of Mississippi		Jackson	Mississippi	38677	US
Ellinor, Patrick	Massachusetts General Hospital		Boston	Massachusetts	02114	US
Emery, Leslie	University of Washington		Seattle	Washington	98195	US
Farber, Charles	University of Virginia		Charlottesville	Virginia	22903	US
Farnam, Leanna	Brigham & Women's Hospital		Boston	Massachusetts	02115	US
Fingerlin, Tasha	National Jewish Health	Center for Genes, Environment and Health	Denver	Colorado	80206	US
Flickinger, Matthew	University of Michigan		Ann Arbor	Michigan	48109	US
Fornage, Myriam	University of Texas Health at Houston		Houston	Texas	77225	US
Franceschini, Nora	University of North Carolina		Chapel Hill	North Carolina	27599	US
Fu, Mao	University of Maryland		Baltimore	Maryland	21201	US
Fullerton, Stephanie M.	University of Washington		Seattle	Washington	98195	US
Fulton, Lucinda	Washington University in St Louis		St Louis	Missouri	63130	US
Gabriel, Stacey	Broad Institute		Cambridge	Massachusetts	02142	US

Gan, Weiniu	National Heart, Lung, and Blood Institute, National Institutes of Health		Bethesda	Maryland	20892	US
Gao, Yan	University of Mississippi		Jackson	Mississippi	38677	US
Gass, Margery	Fred Hutchinson Cancer Research Center		Seattle	Washington	98109	US
Gelb, Bruce	Icahn School of Medicine at Mount Sinai		New York	New York	10029	US
Geng, Xiaoqi (Priscilla)	University of Michigan		Ann Arbor	Michigan	48109	US
Germer, Soren	New York Genome Center		New York	New York	10013	US
Gignoux, Chris	Stanford University		Stanford	California	94305	US
Gladwin, Mark	University of Pittsburgh		Pittsburgh	Pennsylvania	15260	US
Glahn, David	Yale University		New Haven	Connecticut	06520	US
Gogarten, Stephanie	University of Washington		Seattle	Washington	98195	US
Gong, Da-Wei	University of Maryland		Baltimore	Maryland	21201	US
Goring, Harald	University of Texas Rio Grande Valley School of Medicine		San Antonio	Texas	78229	US
Gu, C. Charles	Washington University in St Louis		St Louis	Missouri	63130	US
Guan, Yue	University of Maryland		Baltimore	Maryland	21201	US
Guo, Xiuqing	Los Angeles Biomedical Research Institute		Los Angeles	California	90502	US
Haessler, Jeff	Fred Hutchinson Cancer Research Center, Women's Health Initiative		Seattle	Washington	98109	US

Hall, Michael	University of Mississippi		Jackson	Mississippi	38677	US
Harris, Daniel	University of Maryland		Baltimore	Maryland	21201	US
Hawley, Nicola	Yale University		New Haven	Connecticut	06520	US
He, Jiang	Tulane University		New Orleans	Louisiana	70118	US
Heavner, Ben	University of Washington	Biostatistics	Seattle	Washington	98195	US
Heckbert, Susan	University of Washington		Seattle	Washington	98195	US
Hernandez, Ryan	McGill University, University of California, San Francisco					CA
Herrington, David	Wake Forest Baptist Health		Winston-Salem	North Carolina	27157	US
Hersh, Craig	Brigham & Women's Hospital	Channing Division of Network Medicine	Boston	Massachusetts	02115	US
Hidalgo, Bertha	University of Alabama		Birmingham	Alabama	35487	US
Hixson, James	University of Texas Health at Houston		Houston	Texas	77225	US
Hokanson, John	University of Colorado at Denver		Denver	Colorado	80204	US
Hong, Elliott	University of Maryland		Baltimore	Maryland	21201	US
Hoth, Karin	University of Iowa		Iowa City	Iowa	52242	US
Hsiung, Chao (Agnes)	National Health Research Institute Taiwan	Institute of Population Health Sciences, NHRI	Miaoli County		350	TW
Huston, Haley	Blood Works Northwest		Seattle	Washington	98105	US
Hwu, Chii Min	Taichung Veterans General Hospital Taiwan		Taichung City		407	TW
Irvin, Marguerite Ryan	University of Alabama		Birmingham	Alabama	35487	US

Jackson, Rebecca	Ohio State University Wexner Medical Center	Internal Medicine, DIvision of Endocrinology, Diabetes and Metabolism	Columbus	Ohio	43210	US
Jain, Deepti	University of Washington		Seattle	Washington	98195	US
Jaquish, Cashell	National Heart, Lung, and Blood Institute, National Institutes of Health		Bethesda	Maryland	20892	US
Jhun, Min A	University of Michigan		Ann Arbor	Michigan	48109	US
Johnsen, Jill	Blood Works Northwest, University of Washington		Seattle	Washington	98106	US
Johnson, Andrew	National Heart, Lung, and Blood Institute, National Institutes of Health		Bethesda	Maryland	20892	US
Johnson, Craig	University of Washington		Seattle	Washington	98195	US
Johnston, Rich	Emory University		Atlanta	Georgia	30322	US
Jones, Kimberly	Johns Hopkins University		Baltimore	Maryland	21218	US
Kang, Hyun Min	University of Michigan	Biostatistics	Ann Arbor	Michigan	48109	US
Kaplan, Robert	Albert Einstein College of Medicine		New York	New York	10461	US
Kardia, Sharon	University of Michigan		Ann Arbor	Michigan	48109	US
Kathiresan, Sekar	Broad Institute		Cambridge	Massachusetts	02142	US
Kaufman, Laura	Brigham & Women's Hospital		Boston	Massachusetts	02115	US
Kelly, Shannon	Vitalant Research Institute		San Francisco	California	94118	US
Kenny, Eimear	Icahn School of Medicine at Mount Sinai		New York	New York	10029	US
Kessler, Michael	University of Maryland		Baltimore	Maryland	21201	US

Khan, Alyna	University of Washington		Seattle	Washington	98195	US
Kinney, Greg	University of Colorado at Denver		Denver	Colorado	80204	US
Konkle, Barbara	Blood Works Northwest		Seattle	Washington	98104	US
Kooperberg, Charles	Fred Hutchinson Cancer Research Center		Seattle	Washington	98109	US
Kramer, Holly	Loyola University	Public Health Sciences	Maywood	Illinois	60153	US
Krauter, Stephanie	University of Washington		Seattle	Washington	98195	US
Lange, Christoph	Harvard School of Public Health	Biostats	Boston	Massachusetts	02115	US
Lange, Ethan	University of Colorado at Denver		Denver	Colorado	80204	US
Lange, Leslie	University of Colorado at Denver		Denver	Colorado	80204	US
Laurie, Cathy	University of Washington		Seattle	Washington	98195	US
Laurie, Cecelia	University of Washington		Seattle	Washington	98195	US
LeBoff, Meryl	Brigham & Women's Hospital		Boston	Massachusetts	02115	US
Lee, Jiwon	Brigham & Women's Hospital					
Lee, Seunggeun Shawn	University of Michigan		Ann Arbor	Michigan	48109	US
Lee, Wen-Jane	Taichung Veterans General Hospital Taiwan		Taichung City		407	TW
LeFaive, Jonathon	University of Michigan		Ann Arbor	Michigan	48109	US
Levine, David	University of Washington		Seattle	Washington	98195	US

Levy, Dan	National Heart, Lung, and Blood Institute, National Institutes of Health		Bethesda	Maryland	20892	US
Lewis, Joshua	University of Maryland		Baltimore	Maryland	21201	US
Li, Yun	University of North Carolina		Chapel Hill	North Carolina	27599	US
Lin, Honghuang	Boston University		Boston	Massachusetts	02215	US
Lin, Keng Han	University of Michigan		Ann Arbor	Michigan	48109	US
Lin, Xihong	Harvard School of Public Health					
Liu, Simin	Brown University, Women's Health Initiative	Epidemiology	Providence	Rhode Island	02912	US
Liu, Yongmei	Wake Forest Baptist Health		Winston-Salem	North Carolina	27157	US
Loos, Ruth	Icahn School of Medicine at Mount Sinai		New York	New York	10029	US
Lubitz, Steven	Massachusetts General Hospital		Boston	Massachusetts	02114	US
Lunetta, Kathryn	Boston University		Boston	Massachusetts	02215	US
Luo, James	National Heart, Lung, and Blood Institute, National Institutes of Health		Bethesda	Maryland	20892	US
Mahaney, Michael	University of Texas Rio Grande Valley School of Medicine		Brownsville	Texas	78520	US
Make, Barry	Johns Hopkins University		Baltimore	Maryland	21218	US
Manichaikul, Ani	University of Virginia		Charlottesville	Virginia	22903	US
Manson, JoAnn	Brigham & Women's Hospital		Boston	Massachusetts	02115	US
Margolin, Lauren	Broad Institute		Cambridge	Massachusetts	02142	US

Martin, Lisa	George Washington University		Washington	District of Columbia	20052	US
Mathai, Susan	University of Colorado at Denver		Denver	Colorado	80204	US
Mathias, Rasika	Johns Hopkins University		Baltimore	Maryland	21218	US
McArdle, Patrick	University of Maryland		Baltimore	Maryland	21201	US
McDonald, Merry-Lynn	University of Alabama		Birmingham	Alabama	35487	US
McFarland, Sean	Harvard University		Cambridge	Massachusetts	02138	US
McGarvey, Stephen	Brown University		Providence	Rhode Island	02912	US
McHugh, Caitlin	University of Washington	Biostatistics	Seattle	Washington	98145	US
Mei, Hao	University of Mississippi		Jackson	Mississippi	38677	US
Meyers, Deborah A	University of Arizona		Tucson	Arizona	85721	US
Mikulla, Julie	National Heart, Lung, and Blood Institute, National Institutes of Health		Bethesda	Maryland	20892	US
Min, Nancy	University of Mississippi		Jackson	Mississippi	38677	US
Minear, Mollie	National Heart, Lung, and Blood Institute, National Institutes of Health		Bethesda	Maryland	20892	US
Minster, Ryan L	University of Pittsburgh		Pittsburgh	Pennsylvania	15260	US
Mitchell, Braxton D.	University of Maryland		Baltimore	Maryland	21201	US
Montasser, May E.	University of Maryland		Baltimore	Maryland	21201	US
Musani, Solomon	University of Mississippi	Medicine	Jackson	Mississippi	39213	US

Mwasongwe, Stanford	University of Mississippi		Jackson	Mississippi	38677	US
Mychaleckyj, Josyf C	University of Virginia		Charlottesville	Virginia	22903	US
Nadkarni, Girish	Icahn School of Medicine at Mount Sinai		New York	New York	10029	US
Naik, Rakhi	Johns Hopkins University		Baltimore	Maryland	21218	US
Naseri, Take	Ministry of Health, Government of Samoa		Apia			WS
Natarajan, Pradeep	Broad Institute, Harvard University, Massachusetts General Hospital		Cambridge	Massachusetts	02138	US
Nekhai, Sergei	Howard University		Washington	District of Columbia	20059	US
Nelson, Sarah C.	University of Washington	Biostatistics	Seattle	Washington	98195	US
Nickerson, Deborah	University of Washington		Seattle	Washington	98195	US
North, Kari	University of North Carolina		Chapel Hill	North Carolina	27599	US
O'Connell, Jeff	University of Maryland		Balitmore	Maryland	21201	US
O'Connor, Tim	University of Maryland		Baltimore	Maryland	21201	US
Ochs-Balcom, Heather	University at Buffalo		Buffalo	New York	14260	US
Palmer, Nicholette	Wake Forest Baptist Health	Biochemistry	Winston-Salem	North Carolina	27157	US
Pankow, James	University of Minnesota		Minneapolis	Minnesota	55455	US
Papanicolaou, George	National Heart, Lung, and Blood Institute, National Institutes of Health		Bethesda	Maryland	20892	US

Parker, Margaret	Brigham & Women's Hospital		Boston	Massachusetts	02115	US
Parsa, Afshin	University of Maryland		Baltimore	Maryland	21201	US
Penchev, Sara	National Jewish Health		Denver	Colorado	80206	US
Peralta, Juan Manuel	University of Texas Rio Grande Valley School of Medicine		Edinburg	Texas	78539	US
Perez, Marco	Stanford University		Stanford	California	94305	US
Perry, James	University of Maryland		Baltimore	Maryland	21201	US
Peters, Ulrike	Fred Hutchinson Cancer Research Center, University of Washington		Seattle	Washington	98109	US
Peyser, Patricia	University of Michigan		Ann Arbor	Michigan	48109	US
Phillips, Lawrence S	Emory University		Atlanta	Georgia	30322	US
Phillips, Sam	University of Washington		Seattle	Washington	98195	US
Pollin, Toni	University of Maryland		Baltimore	Maryland	21201	US
Post, Wendy	Johns Hopkins University	Cardiology/Medicine	Baltimore	Maryland	21218	US
Powers Becker, Julia	University of Colorado at Denver	Medicine	Denver	Colorado	80204	US
Preethi Boorgula, Meher	University of Colorado at Denver		Denver	Colorado	80204	US
Preuss, Michael	Icahn School of Medicine at Mount Sinai		New York	New York	10029	US
Prokopenko, Dmitry	Harvard University		Cambridge	Massachusetts	02138	US
Psaty, Bruce	University of Washington		Seattle	Washington	98195	US
Qasba, Pankaj	National Heart, Lung, and Blood Institute,		Bethesda	Maryland	20892	US

	National Institutes of Health					
Qiao, Dandi	Brigham & Women's Hospital		Boston	Massachusetts	02115	US
Qin, Zhaohui	Emory University		Atlanta	Georgia	30322	US
Rafaels, Nicholas	University of Colorado at Denver		Denver	Colorado	80045	US
Raffield, Laura	University of North Carolina	Genetics	Chapel Hill	North Carolina	27599	US
Rao, D.C.	Washington University in St Louis		St Louis	Missouri	63130	US
Rasmussen-Torvik, Laura	Northwestern University		Chicago	Illinois	60208	US
Ratan, Aakrosh	University of Virginia		Charlottesville	Virginia	22903	US
Redline, Susan	Brigham & Women's Hospital		Boston	Massachusetts	02115	US
Reed, Robert	University of Maryland		Baltimore	Maryland	21201	US
Regan, Elizabeth	National Jewish Health		Denver	Colorado	80206	US
Reiner, Alex	Fred Hutchinson Cancer Research Center, University of Washington		Seattle	Washington	98109	US
Reupena, Muagututi‘a Sefuiva	Lutia I Puava Ae Mapu I Fagalele		Apia			WS
Rice, Ken	University of Washington		Seattle	Washington	98195	US
Rich, Stephen	University of Virginia		Charlottesville	Virginia	22903	US
Roden, Dan	Vanderbilt University	Medicine, Pharmacology, Biomedicla Informatics	Nashville	Tennessee	37235	US
Roselli, Carolina	Broad Institute		Cambridge	Massachusetts	02142	US
Rotter, Jerome	Los Angeles Biomedical Research Institute		Los Angeles	California	90502	US

Ruczinski, Ingo	Johns Hopkins University		Baltimore	Maryland	21218	US
Russell, Pamela	University of Colorado at Denver		Denver	Colorado	80204	US
Ruuska, Sarah	Blood Works Northwest		Seattle	Washington	98107	US
Ryan, Kathleen	University of Maryland		Baltimore	Maryland	21201	US
Sabino, Ester Cerdeira	Universidade de Sao Paulo	Faculdade de Medicina	Sao Paulo		01310000	BR
Sakornsakolpat, Phuwanat	Brigham & Women's Hospital		Boston	Massachusetts	02115	US
Salimi, Shabnam	University of Maryland		Baltimore	Maryland	21201	US
Salzberg, Steven	Johns Hopkins University		Baltimore	Maryland	21218	US
Sandow, Kevin	Los Angeles Biomedical Research Institute	TGPS	Torrance	California	90502	US
Sankaran, Vijay	Harvard University		Cambridge	Massachusetts	02138	US
Scheller, Christopher	University of Michigan		Ann Arbor	Michigan	48109	US
Schmidt, Ellen	University of Michigan		Ann Arbor	Michigan	48109	US
Schwander, Karen	Washington University in St Louis		St Louis	Missouri	63130	US
Schwartz, David	University of Colorado at Denver		Denver	Colorado	80204	US
Sciurba, Frank	University of Pittsburgh		Pittsburgh	Pennsylvania	15260	US
Seidman, Christine	Harvard Medical School	Genetics	Boston	Massachusetts	02115	US
Seidman, Jonathan	Harvard Medical School					
Sheehan, Vivien	Baylor College of Medicine	Pediatrics	Houston	Texas	77030	US
Shetty, Amol	University of Maryland		Baltimore	Maryland	21201	US
Shetty, Aniket	University of Colorado at Denver		Denver	Colorado	80204	US

Sheu, Wayne Hui-Heng	Taichung Veterans General Hospital Taiwan		Taichung City		407	TW
Shoemaker, M. Benjamin	Vanderbilt University		Nashville	Tennessee	37235	US
Silver, Brian	UMass Memorial Medical Center		Worcester	Massachusetts	01655	US
Silverman, Edwin	Brigham & Women's Hospital		Boston	Massachusetts	02115	US
Smith, Jennifer	University of Michigan		Ann Arbor	Michigan	48109	US
Smith, Josh	University of Washington		Seattle	Washington	98195	US
Smith, Nicholas	University of Washington		Seattle	Washington	98195	US
Smith, Tanja	New York Genome Center		New York	New York	10013	US
Smoller, Sylvia	Albert Einstein College of Medicine		New York	New York	10461	US
Snively, Beverly	Wake Forest Baptist Health	Biostatistical Sciences	Winston-Salem	North Carolina	27157	US
Sofer, Tamar	Brigham & Women's Hospital		Boston	Massachusetts	02115	US
Sotoodehnia, Nona	University of Washington		Seattle	Washington	98195	US
Stilp, Adrienne	University of Washington		Seattle	Washington	98195	US
Streeten, Elizabeth	University of Maryland		Baltimore	Maryland	21201	US
Su, Jessica Lasky	Brigham & Women's Hospital					
Sung, Yun Ju	Washington University in St Louis		St Louis	Missouri	63130	US
Sylvia, Jody	Brigham & Women's Hospital		Boston	Massachusetts	02115	US
Szpiro, Adam	University of Washington		Seattle	Washington	98195	US

Sztalryd, Carole	University of Maryland		Baltimore	Maryland	21201	US
Taliun, Daniel	University of Michigan		Ann Arbor	Michigan	48109	US
Tang, Hua	Stanford University	Genetics	Stanford	California	94305	US
Taub, Margaret	Johns Hopkins University		Baltimore	Maryland	21218	US
Taylor, Kent D.	Los Angeles Biomedical Research Institute	Institute for Translational Genomics and Populations Sciences	Torrance	California	90502	US
Taylor, Simeon	University of Maryland		Baltimore	Maryland	21201	US
Telen, Marilyn	Duke University		Durham	North Carolina	27708	US
Thornton, Timothy A.	University of Washington		Seattle	Washington	98195	US
Tinker, Lesley	Women's Health Initiative		Seattle	Washington	98109	US
Tirschwell, David	University of Washington		Seattle	Washington	98195	US
Tiwari, Hemant	University of Alabama		Birmingham	Alabama	35487	US
Tracy, Russell	University of Vermont	Pathology & Laboratory Medicine	Burlington	Vermont	05405	US
Tsai, Michael	University of Minnesota		Minneapolis	Minnesota	55455	US
Vaidya, Dhananjay	Johns Hopkins University		Baltimore	Maryland	21218	US
VandeHaar, Peter	University of Michigan		Ann Arbor	Michigan	48109	US
Vasan, Ramachandran S.	Boston University		Boston	Massachusetts	02215	US
Vrieze, Scott	University of Colorado at Boulder, University of Minnesota		Boulder	Colorado	80309	US
Walker, Tarik	University of Colorado at Denver		Denver	Colorado	80204	US
Wallace, Robert	University of Iowa		Iowa City	Iowa	52242	US
Walts, Avram	University of Colorado at Denver		Denver	Colorado	80204	US

Wan, Emily	Brigham & Women's Hospital		Boston	Massachusetts	02115	US
Wang, Fei Fei	University of Washington		Seattle	Washington	98195	US
Wang, Heming	Brigham & Women's Hospital, Partners.org					
Watson, Karol	University of California, Los Angeles		Los Angeles	California	90095	US
Weeks, Daniel E.	University of Pittsburgh		Pittsburgh	Pennsylvania	15260	US
Weir, Bruce	University of Washington		Seattle	Washington	98195	US
Weiss, Scott	Brigham & Women's Hospital		Boston	Massachusetts	02115	US
Weng, Lu-Chen	Massachusetts General Hospital		Boston	Massachusetts	02114	US
Willer, Cristen	University of Michigan	Internal Medicine	Ann Arbor	Michigan	48109	US
Williams, Kayleen	University of Washington		Seattle	Washington	98195	US
Williams, L. Keoki	Henry Ford Health System		Detroit	Michigan	48202	US
Wilson, Carla	Brigham & Women's Hospital		Boston	Massachusetts	02115	US
Wilson, James	University of Mississippi	Department of Physiology and Biophysics	Jackson	Mississippi	39216	US
Wong, Quenna	University of Washington		Seattle	Washington	98195	US
Xu, Huichun	University of Maryland		Baltimore	Maryland	21201	US
Yanek, Lisa	Johns Hopkins University		Baltimore	Maryland	21218	US
Yang, Ivana	University of Colorado at Denver		Denver	Colorado	80204	US
Yang, Rongze	University of Maryland		Baltimore	Maryland	21201	US
Zaghloul, Norann	University of Maryland		Baltimore	Maryland	21201	US
Zekavat, Maryam	Broad Institute		Cambridge	Massachusetts	02142	US

Zhang, Yingze	University of Pittsburgh	Medicine	Pittsburgh	Pennsylvania	15260	US
Zhao, Snow Xueyan	National Jewish Health		Denver	Colorado	80206	US
Zhao, Wei	University of Michigan		Ann Arbor	Michigan	48109	US
Zhi, Degui	University of Texas Health at Houston		Houston	Texas	77225	US
Zhou, Xiang	University of Michigan		Ann Arbor	Michigan	48109	US
Zhu, Xiaofeng	Case Western Reserve University	Department of Population and Quantitative Health Sciences	Cleveland	Ohio	44106	US
Zody, Michael	New York Genome Center		New York	New York	10013	US
Zoellner, Sebastian	University of Michigan		Ann Arbor	Michigan	48109	US

TOPMed Inflammation Working Group

Stella Aslibekyan
Paul Auer
David Beame
Ferdouse Begum
Emelia Benjamin
Joshua Bis
Michael Bowers
Russell Bowler
Erin Buth
Brian Cade
Adolfo Correa
Jeffrey Curtis
Margaret Mengmeng Du
Josee Dupuis
Jon Peter Durda
Nauder Faraday
Ervin Fox
Sheila Gaynor

Rebecca Jackson
Min A Jhun
Anne Justice
Brian Kral
Martin Larson
David Levine
Honghuang Lin
Xihong Lin
Merry-Lynn McDonald
John McLenithan
Michael Mendelson
Julie Mikulla
Nancy Min
Joanne Murabito
Nels Olson
Nathan Pankratz
Ulrike Peters
Linda Polfus
Bruce Psaty
Jenn Purnell
Laura Raffield
Deepa Rastogi
Elizabeth Regan
Alex Reiner
Annabelle Rodriguez
Ester Cerdeira Sabino
Shabnam Salimi
Cassie Spracklen
Ryan Sun
Russell Tracy
Dhananjay Vaidya
Biqi Becky Wang
Fei Fei Wang
Kate Wehr
James Wilson
Lue Ping Zhao